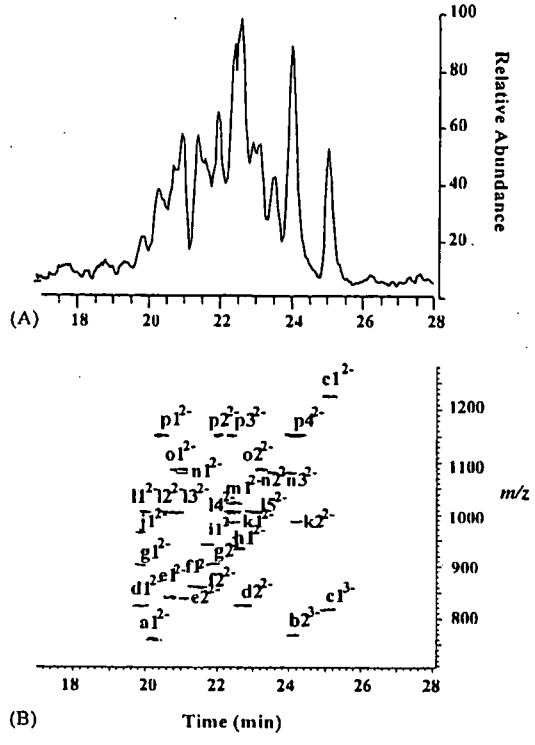

Fig. 6. TIC of a mixture of equal amount of d_0-PA N-linked oligosaccharides from rhCG and d_4-PA N-linked oligosaccharides from hCG (A), and its 2D display (B). Oligosaccharides (from 2 μg rhCG and hCG) were analyzed by GCC-LC/MS in the negative ion mode.

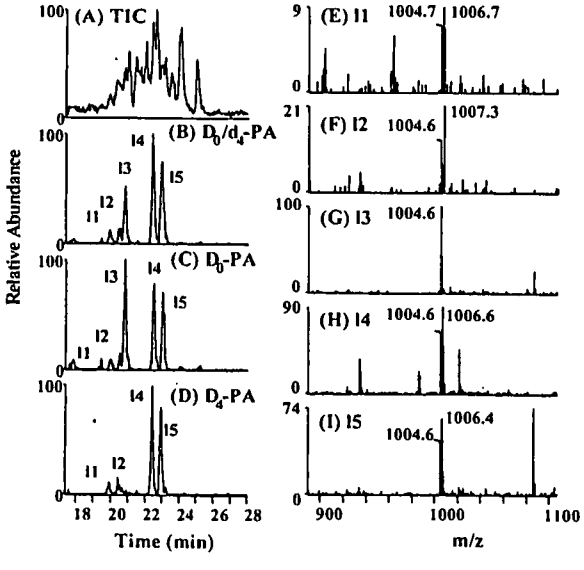

Fig. 7. TIC of a mixture of equal amount of d_0-PA N-linked oligosaccharides from rhCG and d_4-PA N-linked oligosaccharides from hCG (A). Extracted ion chromatograms of d_0-, and d_4-PA monosialylated biantennary (set *m/z* values, 1004–1007) (B), d_0-PA monosialylated biantennary (set *m/z* values, 1004–1005) (C), and d_4-PA monosialylated biantennary oligosaccharides (set *m/z* values, 1006–1007) (D). Mass spectra of peak I1–I5 (E–I).

Fourteen oligosaccharides were detected only in hCG, and most of them were fucosylated complex type. These results show the differences in glycosylation between rhCG and hCG and suggest that many hybrid type oligosaccharides linked to rhCG, while fucosylated oligosaccharides attach to hCG.

4. Discussion

Alteration of glycosylation is known to cause many changes in the biological activity as well as the physical properties of proteins. Several procedures of oligosaccharide profiling have been reported for the assessment of alteration of glycosylation, however, most of them can be used for only either qualitative or quantitative analysis. Although mass spectrometric oligosaccharide profiling is useful for the qualitative analysis, it has a problem on precision, and some isomers are still indistinguishable if their retention times are closed to others. In this study, we demonstrated that the use of isotope-tagged internal standards and GCC-LC/MS made it possible to do both quantitative and qualitative carbohydrate analysis.

First, we demonstrated the monosaccharide composition analysis using the isotope tag method. The use of internal standards that were heated under the same hydrolysis condition as an analyte glycoprotein resulted in good precision and accuracy in the monosaccharide composition analysis. Several HPLC methods for determination of monosaccharides have been reported. High-performance anion-exchange chromatography with pulsed amperometric detection (HPAEC-PAD) has been widely used for monosaccharide composition analysis [20,22–25]. Although HPAEC-PAD gives high resolution of all common monosaccharides and has the advantage of not requiring derivatization, this method is also known to have a disadvantage of limited selectivity [26]. The isotope tag method with SIM mode is equal to the HPAEC-PAD in sensitivity and is better than it in selectivity.

Next, we demonstrated the potentiality of the isotope tag method for quantitative oligosaccharide profiling using rhCG and hCG as model glycoproteins. hCG consists of an α subunit (MW 14.7 kDa) and a β subunit (MW 23.0 kDa), and oligosaccharides link to Asn52, and 78 in the α subunit and Asn13 and 30 in the β subunit. It has been reported that the majority of N-linked oligosaccharides in rhCG and hCG are fucosylated or non-fucosylated di-, tri-, and tetra-antennary forms with a various level of sialylation [27–30]. We prepared d_0-PA oligosaccharides and d_4-PA oligosaccharides from rhCG and hCG, respectively, and an equal part of d_0-PA and d_4-PA oligosaccharides was injected into LC/MS. We demonstrated that the oligosaccharides existing in one side protein were detected as single ions, whereas common oligosaccharides were detected as paired ions. We could easily realize that monosialo-, and disialobiantennary oligosaccharides linked to both hCG and rhCG, while fucosylated oligosaccharides and some hybrid type oligosaccharides linked to only hCG and rhCG, respectively. In addition, we demonstrated the pos-

sibility of the quantitative comparison the oligosaccharides between two quite similar glycoproteins. This quantitative oligosaccharide profiling is expected to be a powerful tool in various stages, including quality control and comparability assessment of glycoprotein products, and elucidation of glycan alteration in some diseases.

Acknowledgements

This study was supported in part by the Japan–China Sasakawa Medical Fellowship (J.Y.) and by a grant-in-aid for Research on Health Sciences focusing on Drug Innovation from The Japan Health Sciences Foundation (N.K.).

References

[1] A. Varki, Glycobiology 3 (1993) 97.
[2] T. Hayakawa, in: Y.-y.H. Chiu, J.L. Gueriguian (Eds.), Drug Biotechnology Regulation. Scientific Basis and Practices, Marcel Dekker Inc., New York, 1991, p. 468.
[3] N. Takahashi, H. Nakagawa, K. Fujikawa, Y. Kawamura, N. Tomiya, Anal. Biochem. 226 (1995) 139.
[4] R.R. Townsend, M.R. Hardy, O. Hindsgaul, Y.C. Lee, Anal. Biochem. 174 (1988) 459.
[5] G.R. Guile, P.M. Rudd, D.R. Wing, S.B. Prime, R.A. Dwek, Anal. Biochem. 240 (1996) 210.
[6] L. Royle, T.S. Mattu, E. Hart, J.I. Langridge, A.H. Merry, N. Murphy, D.J. Harvey, R.A. Dwek, P.M. Rudd, Anal. Biochem. 304 (2002) 70.
[7] J. Delaney, P. Vouros, Rapid Commun. Mass Spectrom. 15 (2001) 325.
[8] K.A. Thomsson, H. Karlsson, G.C. Hansson, Anal. Chem. 72 (2000) 4543.
[9] N. Kawasaki, M. Ohta, S. Hyuga, M. Hyuga, T. Hayakawa, Anal. Biochem. 285 (2000) 82.
[10] N. Kawasaki, S. Itoh, M. Ohta, T. Hayakawa, Anal. Biochem. 316 (2003) 15.
[11] N. Kawasaki, M. Ohta, S. Itoh, M. Hyuga, S. Hyuga, T. Hayakawa, Biologicals 30 (2002) 113.
[12] S.P. Gygi, B. Rist, S.A. Gerber, F. Turecek, M.H. Gelb, R. Aebersold, Nat. Biotechnol. 17 (1999) 994.
[13] S. Hase, T. Ikenaka, Y. Matsushima, Biochem. Biophys. Res. Commun. 85 (1978) 257.
[14] S. Hase, S. Hara, Y. Matsushima, J. Biochem. (Tokyo) 85 (1979) 217.
[15] S. Suzuki, K. Kakehi, S. Honda, Anal. Chem. 68 (1996) 2073.
[16] M. Wuhrer, H. Geyer, M. von der Ohe, R. Gerardy-Schahn, M. Schachner, R. Geyer, Biochimie 85 (2003) 207.
[17] S. Itoh, N. Kawasaki, M. Ohta, T. Hayakawa, J. Chromatogr. A 978 (2002) 141.
[18] J.Q. Fan, Y. Namiki, K. Matsuoka, Y.C. Lee, Anal. Biochem. 219 (1994) 375.
[19] H. Takemoto, S. Hase, T. Ikenaka, Anal. Biochem. 145 (1985) 245.
[20] M.R. Hardy, R.R. Townsend, Y.C. Lee, Anal. Biochem. 170 (1988) 54.
[21] H. Sasaki, B. Bothner, A. Dell, M. Fukuda, J. Biol. Chem. 262 (1987) 12059.
[22] M.R. Hardy, Methods Enzymol. 179 (1989) 76.
[23] C.C. Ip, V. Manam, R. Hepler, J.P. Hennessey Jr., Anal. Biochem. 201 (1992) 343.
[24] A. Lampio, J. Finne, Anal. Biochem. 197 (1991) 132.
[25] Y.C. Lee, Anal. Biochem. 189 (1990) 151.
[26] M. Weitzhandler, C. Pohl, J. Rohrer, L. Narayanan, R. Slingsby, N. Avdalovic, Anal. Biochem. 241 (1996) 128.
[27] A. Kobata, J. Cell Biochem. 37 (1988) 79.
[28] Y. Endo, K. Yamashita, Y. Tachibana, S. Tojo, A. Kobata, J. Biochem. (Tokyo) 85 (1979) 669.
[29] A. Amoresano, R. Siciliano, S. Orru, R. Napoleoni, V. Altarocca, E. De Luca, A. Sirna, P. Pucci, Eur. J. Biochem. 242 (1996) 608.
[30] A. Gervais, Y.A. Hammel, S. Pelloux, P. Lepage, G. Baer, N. Carte, O. Sorokine, J.M. Strub, R. Koerner, E. Leize, A. Van Dorsselaer, Glycobiology 13 (2003) 179.

Proteomics 2005, *5*, 4665–4672 DOI 10.1002/pmic.200401330

REGULAR ARTICLE

Glycomic/glycoproteomic analysis by liquid chromatography/mass spectrometry: Analysis of glycan structural alteration in cells

Noritaka Hashii, Nana Kawasaki, Satsuki Itoh, Mashashi Hyuga, Toru Kawanishi and Takao Hayakawa

Division of Biological Chemistry and Biologicals, National Institute of Health Sciences, Tokyo

The alteration of glycosyltransferase expression and the subsequent changes in oligosaccharide structures are reported in several diseases. The analysis of glycan structural alteration in glycoproteins is becoming increasingly important in the discovery of therapies and diagnostic markers. In this study, we propose a strategy for glycomic/glycoproteomic analysis based on oligosaccharide profiling by LC/MS followed by proteomic approaches, including 2-DE and 2-D lectin blot. As a model of aberrant cells, we used Chinese hamster ovary cells transfected with *N*-acetylglucosaminyltransferase III (GnT-III), which catalyzes the addition of a bisecting *N*-acetylglucosamine (GlcNAc) to β-mannose of the mannosyl core of *N*-linked oligosaccharides. LC/MS equipped with a graphitized carbon column (GCC) enabled us to elucidate the structural alteration induced by the GnT-III expression. Using 2-D lectin blot followed by LC/MS/MS, the protein carrying an extra *N*-acetylhexosamine in cells transfected with GnT-III was successfully identified as integrin α3. Thus, oligosaccharide profiling by GCC-LC/MS followed by proteomic methods can be a powerful tool for glycomic/glycoproteomic analysis.

Received: September 20, 2004
Revised: April 22, 2005
Accepted: April 22, 2005

Keywords:
2DE / LC/MS / Lectin blotting / Oligosaccharides profiling

1 Introduction

It is common knowledge that approximately 50% of proteins in mammalian cells are glycosylated and that glycans play crucial roles in various biological events including cell recognition [1], adhesion [2] and cell-cell interaction [3]. The alteration of glycosyltransferase expression and subsequent changes in oligosaccharide structures are reported in several diseases, including inherited diseases [4], the progression of cancer [5] and autoimmune diseases [6–8]. The analysis of glycan structural alteration in glycoproteins is becoming increasingly important in the discovery of therapies and diagnostic markers.

Comprehensive analysis of proteins in a given cellular sample is the most effective means of elucidating the disease mechanism. Simultaneous separation and characterization of proteins by 2-DE and 2-D LC followed by MS have been utilized as the fundamental approaches to proteomic analysis; however, these approaches alone are ineffectual for the elucidation of the glycan structural alteration in glycoproteins. A strategy based on qualitative and quantitative glycomic analysis is necessary for the study of glycosylation-associated diseases.

LC/MS is widely used for glycosylation analysis in glycoproteins. Previously, we demonstrated that LC/MS equipped with a graphitized carbon column (GCC-LC/MS) is a useful means of oligosaccharide profiling and for the structural analysis of carbohydrates [9–12]. Using this method, oligosaccharides, including high mannose, hybrid and complex

Correspondence: Dr. Nana Kawasaki, 1-18-1, Kamiyoga, Setagaya-ku, Tokyo, 158-8501, Japan
E-mail: nana@nihs.go.jp
Fax: +81-3-3700-9084

Abbreviations: CHO, Chinese hamster ovary; **CHO-III cells**, CHO cells transfected with *N*-acetylglucosaminyltransferase III; **dHex**, deoxyhexose; **GCC**, graphitized carbon column; **GlcNAc**, *N*-acetylglucosamine; **GnT-III**, *N*-acetylglucosaminyltransferase III; **Hex**, hexose; **HexNAc**, *N*-acetylhexosamine; **NeuAc**, *N*-acetylneuraminic acid; **PNGase F**, peptide *N*-glycosidase F

types with or without sialic acids, can be separated, and structural information can be obtained from their mass spectra and chromatographic behavior.

Here we propose a strategy for performing glycomic/glycoproteomic analysis based on a combination of GCC-LC/MS and proteomic approaches.

First, GCC-LC/MS is applied to the analysis of oligosaccharide structural alteration in aberrant cells. Chinese hamster ovary (CHO) cells, used as a model of aberrant cells, were transfected with *N*-acetylglucosaminyltransferase III (GnT-III), which catalyzes the addition of bisecting *N*-acetylglucosamine (GlcNAc) to the trimannosyl core of *N*-linked oligosaccharides [13] and is associated with cell adhesion [14] and the suppression of tumor cell metastasis [15–17]. Then, 2-D lectin blotting followed by LC/MS/MS was used to identify the protein in which glycosylation was altered by the expression of GnT-III.

2 Materials and methods

2.1 Cell lines and culture

The CHO cells were obtained from the Japanese Collection of Research Bioresources (Tokyo, Japan). The human GnT-III cDNA was cloned into the pCI-neo vector. The expression vector was transfected into CHO cells with LipofectAMINE plus reagent, according to the manufacturer's instructions. To screen the transformants, the transfectants were cultured with Ham's F12 medium supplemented with 10% fetal calf serum (FCS) and 1 mg/mL G418. After 2 weeks, the colonies were lifted with a micropipette. A high GnT-III-expressing clone was used in succeeding experiments.

The CHO cells and GnT-III-transfected CHO cells (CHO-III cells) were cultured in Ham's F12 medium supplemented with 10% FCS, 100 U/mL of penicillin and 100 μg/mL of streptomycin under a humidified atmosphere of 95% air and 5% CO_2. After harvesting CHO and CHO-III cells, they were rinsed with PBS containing protease inhibitors and 2 mM EDTA.

2.2 Preparation of insoluble and soluble fractions

The insoluble and soluble fractions were prepared from CHO and CHO-III cells using a Mem-PER Eukaryotic Membrane Protein Extraction Reagent Kit (Pierce Biotechnology, P.O., USA). The detergent in these fractions was removed with Detergent-OUT (Geno Technology, M.O., USA) three times. For desalting and degreasing, seven volumes of acetone were added to the sample solution, and the mixture was stirred and sonicated. The mixture was then incubated at −20°C for 1 h and centrifuged at 4°C for 15 min, 15 000 × g. The supernatants were discarded, and the pellets dried. The protein concentrations were determined using a BCA protein assay kit (Pierce).

2.3 Preparation of *N*-linked oligosaccharide alditols

The protein (500 μg) from each fraction was dissolved in 810 μL of 0.5 M Tris-HCl containing 8 M guanidine-HCl and 5 mM EDTA (pH 8.6), and then 6.0 μL of 2-mercaptoethanol were added in the solution. After incubation at room temperature for 2 h, freshly prepared 0.6 M sodium monoiodoacetamide (135 μL) was added to the solution. After incubation at room temperature for 2 h in the dark, the solution was desalted with PD10 column (Amersham Biosciences, NJ, USA), and the elute was lyophilized. The carboxylmethylated proteins were dissolved in 500 μL of 100 mM PBS (pH 7.2), and 20 U of peptide *N*-glycosidase F (PNGase F) (Roche Diagnostics, Mannheim, Germany) were added to the solution. After incubation at 37°C for 4 days, 1.74 mL of cold ethanol was added to the solution, the mixture was incubated at −20°C for 3 h, and proteins were removed by centrifugation at 4°C for 10 min (15 000 × g). The supernatants containing oligosaccharides were evaporated, and then lyophilized. The oligosaccharides were incubated with 500 μL of 0.5 M $NaBH_4$ at room temperature for 16 h, and then neutralized with 10% (v/v) acetic acid to pH 6.5 and desalted with Envi-Carb (Supelco, Bellefonte, USA).

2.4 GCC-LC/MS

LC was carried out using a MAGIC 2002 system (Michrom BioResources, Auburn, CA, USA). The GCC used was a Hypercarb column (150 × 0.2 mm, ThermoFinnigan, San Jose, CA, USA). The eluents were 5 mM ammonium acetate, pH 8.5, containing 2% ACN (pump A) and 5 mM ammonium acetate, pH 8.5, containing 80% ACN (pump B). The borohydride-reduced oligosaccharides were eluted at a flow rate of 2 μL/min with a gradient of 10–45% of pump B in 90 min. Mass spectra were recorded on a TSQ 7000 triple-stage quadruple mass spectrometer (ThermoFinnigan) equipped with a nanoelectorospray ion source (AMR, Inc., Tokyo, Japan). The mass spectrometer was operated in positive ion mode. Ions in the range of *m/z* 900–2400 were acquired with a scan duration of 3 s. The ESI voltage was set at 2.0 kV, and the capillary temperature was 175°C. The electron multiplier was set at 1.0 kV. Collisions for MS/MS were carried out with collision energy of 25%, scan duration of 4 s., and mass range of *m/z* 100–2000.

2.5 1-D SDS-PAGE and lectin blotting

Proteins were separated by 1-D SDS-PAGE (12.5% T, 3% C) as described by Laemmli [18] and stained with SYPRO Orange (Bio-Rad, Richmond, CA, USA) at room temperature for 30 min in transfer buffer (25 mM Tris-HCl, 20 mM glycine and 20% methanol). The gel images were scanned on a Tyhoon 9400 (Amersham Biosciences) at an excitation wavelength of 540/25 nm and an emission wavelength of 590/30 nm. After saving the gel image, the proteins were blotted to a PVDF membrane (Immun-Blot PVDF membrane,

0.2 μm, Bio-Rad) at 3.0 mA/cm², 20 V for 30 min in transfer buffer containing 0.1% SDS using a semi-dry blotter (Trans-blot SD sel, Bio-Rad). The efficiency and position of the transfer were confirmed using SYPRO Orange transferred together with proteins. Nonspecific sites on the membrane were blocked at 4°C for 16 h in 0.5% casein-PBS. After the membranes were washed with 0.05% Tween-PBS (T-PBS) three times, they were treated with 0.1 U/mL of sialidase (Nacalai Tesque, Kyoto, Japan) at 37°C for 16 h in 0.5 M acetate buffer (pH 5.0). The membranes were then re-blocked with 0.5% casein-PBS at 37°C for 15 min, washed with T-PBS three times, and incubated with biotinylated phytohemagglutinin-E4 (PHA-E4, 2 μg/mL) at 4°C for 2 h in PBS (pH 7.4). The membranes were then washed with T-PBS and incubated with 1:1000 diluted avidin-alkaline phosphatase (AP) complex solution at 4°C for 1 h in PBS.

2.6 Concentration of target proteins in the gel

The band detected by lectin blotting on 1-D gel was excised and then mashed in 20 mM Tris-HCl (pH 8.0) containing 2% SDS. The proteins in the gel particles were extracted by intermittent sonication at 4°C for 30 min, followed by shaking at room temperature for 16 h. After extraction, the gel particles were removed by centrifugation (15 000 × g). The proteins in the supernatant were precipitated with sevenfold acetone at −20°C for 3 h, and then the precipitates were washed with acetone three times to remove salts and detergent.

2.7 2-DE

For first dimension IEF of the sample, Immobiline DryStrip gel (13 cm, pH4–7 NL, Amersham Biosciences) was used. The samples were dissolved in IEF solution containing 7 M urea, 2 M thiourea, 18 mM DTT, 0.5% IPG buffer, 2% CHAPS, and bromophenol blue. Dried IPG strips were rehydrated overnight in the sample solution. IEF was then performed using the following steps: 500 V for 1 h, 100 V for 1 h, and 8000 V for 2 h, *i.e.* a total of 17.5 kVh.

IPG strips were treated with 10 mL of 50 mM Tris-HCl (pH 8.8) containing 2% SDS, 6 M urea, 30% glycerol and 65 mM DTT for 15 min, and then treated with 10 mL of 50 mM Tris-Cl (pH 8.8) containing 2% SDS, 6 M urea, 30% glycerol and 135 mM iodoacetamide for 15 min in order to reduce the disulfide bonds of cysteinyl residues. SDS-polyacrylamide gels (7.5%T, 3%C, size 140 × 140 × 1 mm) and running buffer containing 25 mM Tris-HCl, 192 mM glycine and 0.1% SDS were used for the 2-DE. The gels were run at 25 mA/gel after setting the IPG strip on the gel. Fluorescent staining and scanning of gel, followed by lectin blotting, were performed as mentioned above. In 2-D lectin blotting, the proteins were blotted to a PVDF membrane at 3.0 mA/cm², 20 V for 90 min.

2.8 In-gel digestion and protein identification by LC/MS/MS

Interesting spots were excised from the 2-DE gel for in-gel trypsin digestion. The gel particles were destained with 20 mM ammonium bicarbonate containing 50% methanol in microcentrifuge tubes, and dehydrated in 100% ACN. Enzymatic digestion was performed overnight at 37°C with 5 μL of 20 μg/mL trypsin (Promega, Madison, WI, USA) in 20 mM ammonium bicarbonate (pH 8.5). Digested peptides were extracted with 1% TFA in 50% ACN, and samples were dried with a Speed-Vac and redissolved in 0.1% TFA for LC/MS.

LC was carried out using a Paradigm MS4 (Michrom BioResources) equipped with Magic C18 column (50 × 0.2 mm, Michrom BioResources). The eluents were 0.1% formic acid containing 2% ACN (pump A), and 0.1% formic acid containing 90% ACN (pump B). The peptides were eluted at a flow rate of 2 μL/min with a gradient of 5–70% of pump B in 30 min. Mass spectra were recorded on an API QSTAR Pulsar i (Applied Biosystems, Foster City, CA, USA) in the positive ion mode. The proteins were identified by searching the Swiss-Prot database using MASCOT (Matrix Science, UK). The mass range and MS/MS range were *m/z* 400–2000 and *m/z* 100–2000, respectively, and the ESI voltage was set at 2.5 kV.

3 Results

3.1 Analysis of glycans in the insoluble fractions

N-linked oligosaccharides were released from soluble and insoluble fractions by PNGase F and reduced with $NaBH_4$ to prevent the separation of anomers by GCC. Figure 1A shows the *N*-linked oligosaccharide profile of the insoluble fraction from CHO cells (5×10^7). Diverse oligosaccharide ions were detected by full scan in the positive ion mode of MS. Oligosaccharides were numbered with the labels on peaks where they were detected, and the multiple oligosaccharides in single peak were classified by the digits behind alphabets, such as peaks A1 and A2. Their monosaccharide compositions were deduced from the *m/z* values as shown in Table 1. *N*-linked oligosaccharides from CHO cells have a high proportion of high mannose-type and bi-, tri- and tetra-antennary complex type oligosaccharides [19, 20]. High mannose-type oligosaccharides, $[Man]_{5-9}[GlcNAc]_2$ were detected at 9–23 min (peaks A–E and K). Major components (peaks N2, Q2, R1, S1, T1, U1 and V2) were deduced as fucosylated and non-fucosylated biantennary forms with mono- and di-sialic acids from previous articles and their monosaccharide compositions. Various oligosaccharides, including mono- (peak N1 and Q1), tri- (peak P1, U2, V1), tetra-antennary (peak V3), and hybrid-type (peak F1 and I1) oligosaccharides were detected as minor components together with low molecular weight oligosaccharides such as the trimannosyl core (peaks G1 and O1).

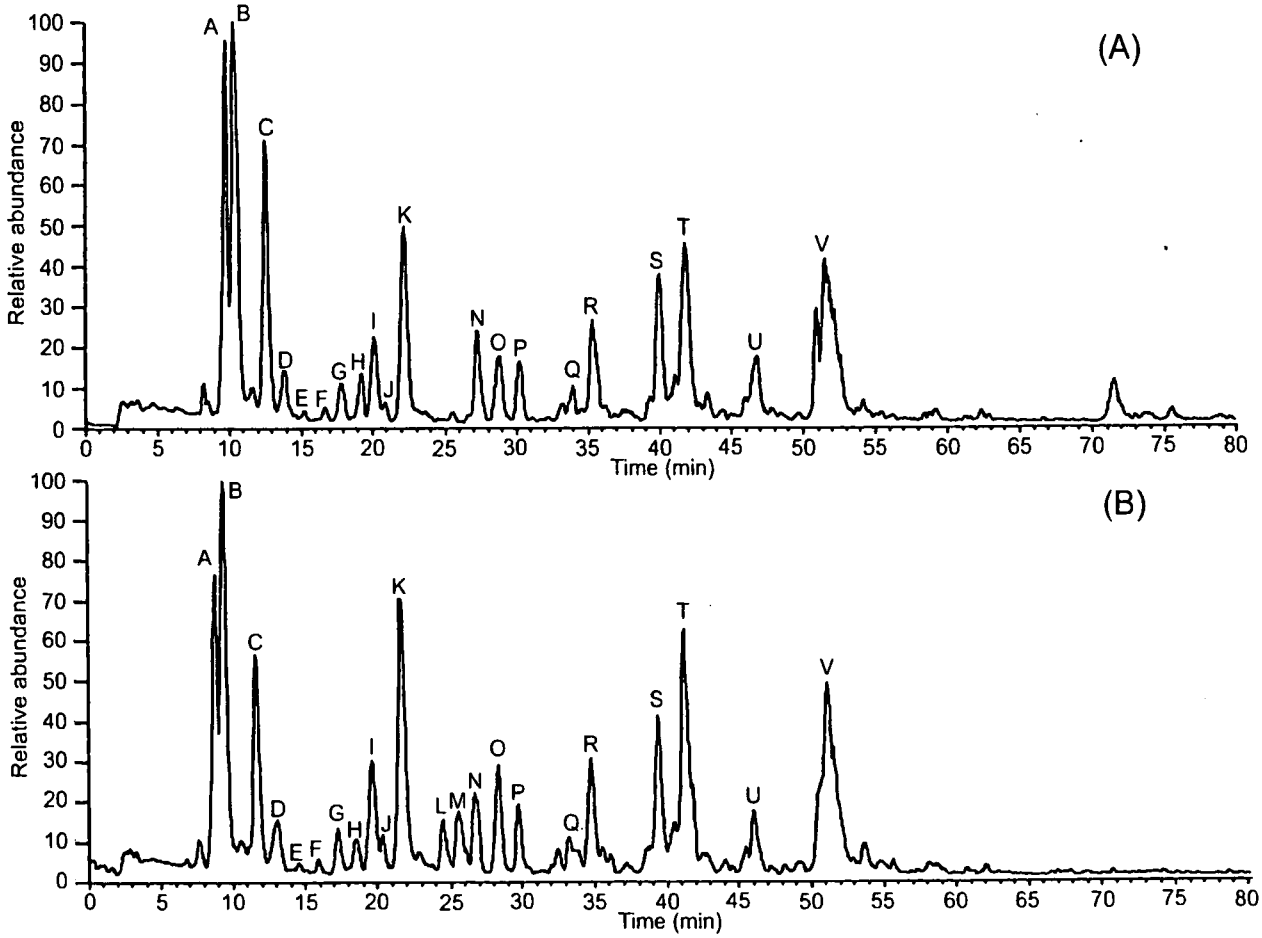

Figure 1. Total ion chromatograms of GCC-LC/MS of borohydride-reduced *N*-linked oligosaccharides released from insoluble fraction of CHO (A) and CHO-III (B) in positive ion mode. Pump A: 5 mM ammonium acetate, pH 8.5, containing 2% ACN. Pump B: 5 mM ammonium acetate, pH 8.5, containing 80% ACN. The borohydride-reduced oligosaccharides were eluted at a flow rate of 2 μL/min with a gradient of 10–45% of pump B in 90 min.

Figure 1B shows the oligosaccharide profile of the CHO-III-insoluble fraction. The distribution of oligosaccharides in CHO-III was different from that in the CHO cell insoluble fraction. Some additional peaks (peaks L1 and M1) were detected in the CHO-III-insoluble fraction, and their doubly charged ions at *m/z* 1143.2 and 1143.0 were consistent with the theoretical *m/z* values of fucosylated biantennary-bearing NeuAc with one additional HexNAc. Figure 2 shows the MS/MS spectrum of peak M1. Detection of $B_{1\gamma}/Y_6^{2+}$ at *m/z* 894.1 and an intense ion of $[HexNAc]^+$, at *m/z* 204 suggest that the oligosaccharide (peak M1) carries one GlcNAc at either of the non-reducing ends. Peak M1 is possibly assigned to bisected biantennary form. In addition, peaks D1, I2 and S2, which were not found in the profile of CHO, were detected in that of CHO-III (Fig. 1B). They can also be deduced as bisected biantennary forms from their MS/MS spectra. Other than these oligosaccharides bearing GlcNAc at either of the non-reducing ends in CHO-III cells, there was no significant difference in glycosylation between CHO and CHO-III cells. These results suggest that only limited oligosaccharides are altered by the expression of GnT-III.

3.2 Analysis of glycans in the soluble fractions

Figure 3A and B shows the *N*-linked oligosaccharide profiles of the soluble fractions of CHO and CHO-III, respectively. The oligosaccharide components of soluble fractions are very different from those of insoluble fractions (Table 1). High mannose-type oligosaccharides, $[Man]_{5-9}[GlcNAc]_2$, were detected as major components (peaks A–C and K), and complex-type and hybrid-type oligosaccharides were detected as minor oligosaccharides in the soluble fraction. Oligosaccharides bearing extra GlcNAc (D1, L1 and M1) were also detected in the soluble fraction of CHO-III.

Table 1. Observed *m/z* values and carbohydrate compositions of peaks A-V in total ion chromatogram 3 of CHO-insoluble (Fig. 1A), CHO-III-insoluble (Fig. 1B), CHO-soluble (Fig. 3A) and CHOIII-soluble (Fig. 3B) fractions

Carbohydrate composition[a]	Theoretical mass[b]	Peak No.		Insoluble fraction				Soluble fraction			
				CHO		CHO-III		CHO		CHO-III	
				Charge state	Observed *m/z*	Charge state	Observed *m/z*	Charge state	Observed *m/z*	Charge state	Observed *m/z*
$[Hex]_7[HexNAc]_2$	1561.4	A	A1	H^+	1562.2	H^+	1562.0	Na^+	1584.4	Na^+	1584.2
$[Hex]_8[HexNAc]_2$	1723.5		A2	Na^+	1746.3	Na^+	1746.3	Na^+	1746.5	Na^+	1746.1
$[Hex]_9[HexNAc]_2$	1885.7	B	B1	Na^+	1908.4	Na^+	1908.5	Na^+	1908.4	Na^+	1908.9
$[Hex]_6[HexNAc]_2$	1399.3	C	C1	H^+	1400.1	H^+	1400.0	H^+	1399.7	H^+	1399.9
$[Hex]_7[HexNAc]_2$	1561.4		C2	Na^+	1584.2	Na^+	1584.0	Na^+	1584.8	Na^+	1584.0
$[dHex]_1[Hex]_5[HexNAc]_5$	1992.9	D	D1		N.D.[c]	$2H^+$	**997.4**		N.D.	$2H^+$	**997.5**
$[Hex]_6[HexNAc]_2$	1399.3		D2	Na^+	1422.0	Na^+	1421.9		N.D.		N.D.
$[Hex]_7[HexNAc]_2$	1561.4		D3	Na^+	1584.2	Na^+	1584.1		N.D.		N.D.
$[Hex]_8[HexNAc]_2$	1723.5		D4	Na^+	1746.2	Na^+	1746.4		N.D.		N.D.
$[Hex]_4[HexNAc]_2$	1075.0	E	E1	Na^+	1097.9	Na^+	1097.6		N.D.		N.D.
$[Hex]_6[HexNAc]_2$	1399.3		E2	H^+	1400.1	H^+	1400.0		N.D.		N.D.
$[Hex]_6[HexNAc]_3$	1602.5	F	F1	H^+	1604.0	H^+	1603.1		N.D.		N.D.
$[Hex]_3[HexNAc]_2$	912.8	G	G1	H^+	913.7	H^+	913.7	Na^+	935.7	Na^+	935.6
$[Hex]_5[HexNAc]_4$	1643.5	H	H1	H^+	1644.5	H^+	1644.2	Na^+	1666.3	Na^+	1666.4
$[Hex]_6[HexNAc]_4$	1827.6	I	I1	$2Na^+$	914.7	$2Na^+$	914.7		N.D.		N.D.
$[Hex]_5[HexNAc]_5[NeuAc]_1$	2137.9		I2		N.D.	$2H^+$	**1069.8**		N.D.		N.D.
$[dHex]_1[Hex]_3[HexNAc]_4$	1465.4	J	J1	H^+	1466.1	H^+	1466.1	Na^+	1488.2	Na^+	1487.9
$[Hex]_5[HexNAc]_2$	1237.1	K	K1	H^+	1238.0	H^+	1238.0	H^+	1237.9	H^+	1237.9
$[dHex]_1[Hex]_5[HexNAc]_5[NeuAc]_1$	2284.1	L	L1		N.D.	$2H^+$	**1143.2**		N.D.	$2H^+$	**1142.9**
$[dHex]_1[Hex]_5[HexNAc]_5[NeuAc]_1$	2284.1	M	M1		N.D.	$2H^+$	**1143.0**		N.D.	$2H^+$	**1143.3**
$[dHex]_1[Hex]_4[HexNAc]_3$	1424.3	N	N1	H^+	1425.4	H^+	1425.3	Na^+	1447.1	Na^+	1447.1
$[dHex]_1[Hex]_5[HexNAc]_4$	1789.7		N2	H^+	1790.1	H^+	1790.3	Na^+	1812.3	Na^+	1812.1
$[dHex]_1[Hex]_3[HexNAc]_2$	1059.0	O	O1	H^+	1059.7	H^+	1059.7	H^+	1059.8	H^+	1059.7
$[dHex]_1[Hex]_6[HexNAc]_5$	2155.0	P	P1	$2H^+$	1078.5	$2H^+$	1078.5		N.D.		N.D.
$[dHex]_1[Hex]_3[HexNAc]_3$	1262.2	Q	Q1	H^+	1263.0	H^+	1263.0		N.D.		N.D.
$[Hex]_5[HexNAc]_4[NeuAc]_1$	1934.7		Q2	$2H^+$	968.4	$2H^+$	968.4		N.D.		N.D.
$[Hex]_5[HexNAc]_4[NeuAc]_1$	1934.7	R	R1	$2H^+$	968.4	$2H^+$	968.4	$2H^+$	968.7	$2H^+$	968.2
$[dHex]_1[Hex]_5[HexNAc]_4[NeuAc]_1$	2080.9	S	S1	$2H^+$	1041.4	$2H^+$	1041.4	$2H^+$	1041.4	$2H^+$	1041.3
$[dHex]_1[Hex]_5[HexNAc]_5[NeuAc]_2$	2574.0		S2		N.D.	$2H^+$	**1288.5**		N.D.		N.D.
$[dHex]_1[Hex]_5[HexNAc]_4[NeuAc]_1$	2080.9	T	T1	$2H^+$	1041.4	$2H^+$	1041.5	$2H^+$	1041.4	$2H^+$	1041.3
$[Hex]_5[HexNAc]_4[NeuAc]_2$	2226.0	U	U1	$2H^+$	1114.0	$2H^+$	1113.9	$2H^+$	1113.9	$2H^+$	1113.9
$[dHex]_1[Hex]_6[HexNAc]_5[NeuAc]_1$	2446.2		U2	$2H^+$	1224.2	$2H^+$	1224.3	$2Na^+$	1124.9		N.D.
$[dHex]_1[Hex]_6[HexNAc]_5[NeuAc]_2$	2737.5	V	V1	$2H^+$	1370.0	$2H^+$	1370.0		N.D.		N.D.
$[dHex]_1[Hex]_5[HexNAc]_4[NeuAc]_2$	2372.1		V2	$2H^+$	1187.1	$2H^+$	1187.1	$2H^+$	1187.2	$2H^+$	1187.2
$[dHex]_1[Hex]_7[HexNAc]_6[NeuAc]_1$	2811.6		V3	$2H^+$	1406.8	$2H^+$	1406.6		N.D.		N.D.

The characteristic *m/z* values observed in total ion chromatograms of CHO-III are depicted in bold type.

a) [dHex], deoxyhexose; [Hex], hexose; [HexNAc], *N*-acetylhexosamine; [NeuAc], *N*-acetylneuraminic acid.

b) Monoisotopic mass values.

c) Not detected.

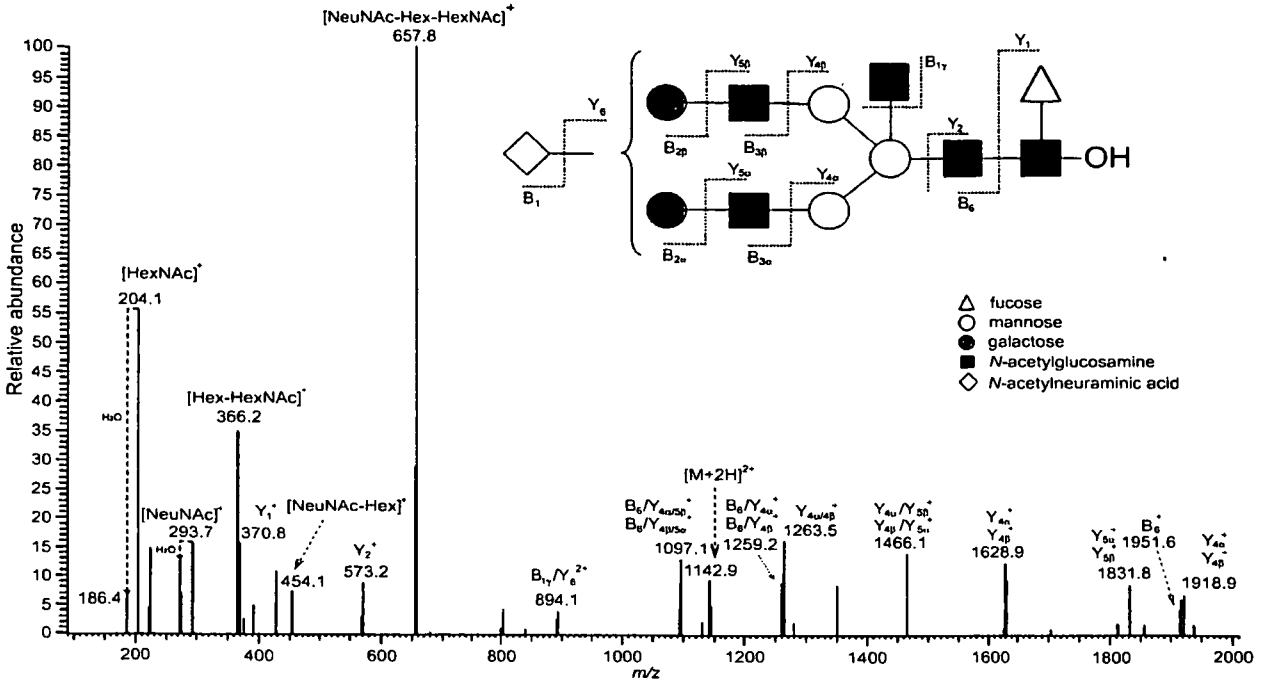

Figure 2. MS/MS spectrum of fucosylated biantennary *N*-linked oligosaccharide (peak M1) detected in the insoluble fraction from CHO-III.

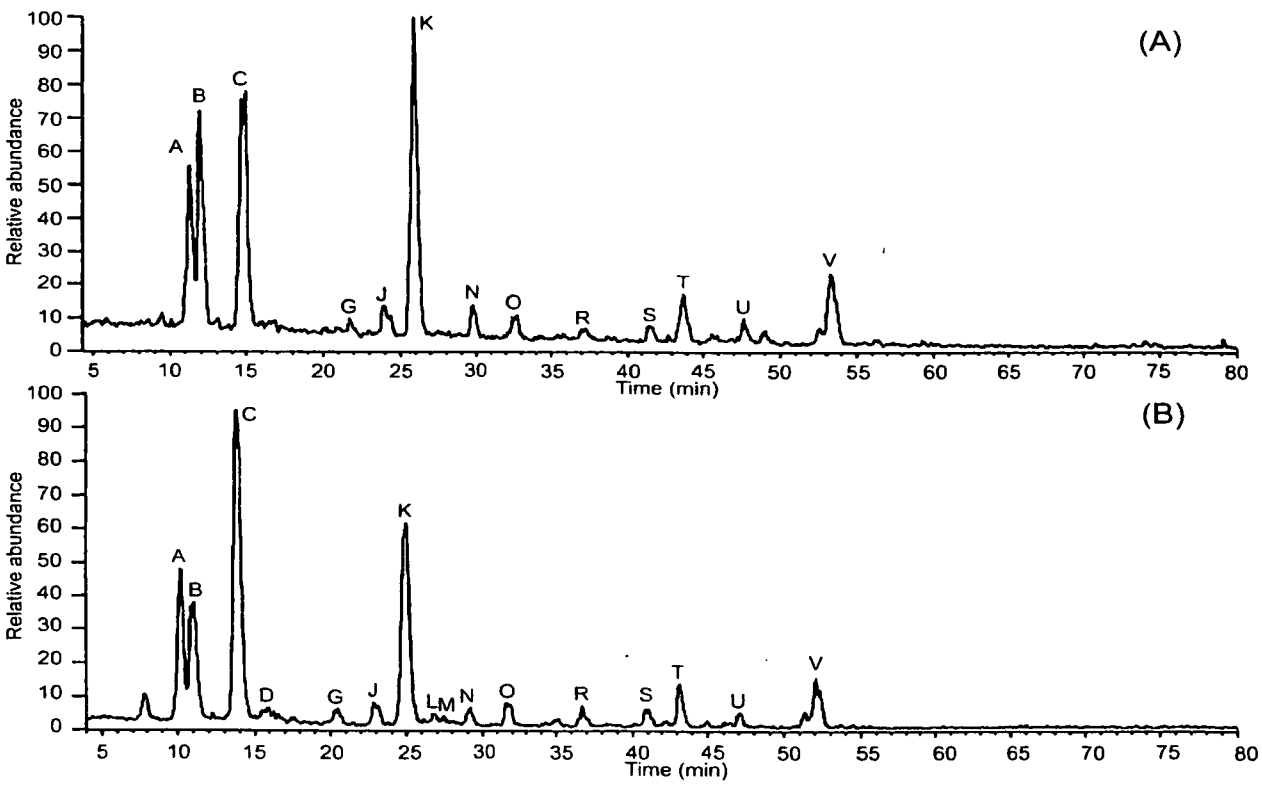

Figure 3. Total ion chromatograms of GCC-LC/MS of borohydride-reduced *N*-linked oligosaccharides released from the soluble fractions of CHO (A) and CHO-III (B) in positive ion mode. Pump A: 5 mM ammonium acetate, pH 8.5, containing 2% ACN. Pump B: 5 mM ammonium acetate, pH 8.5, containing 80% ACN. The borohydride-reduced oligosaccharides were eluted at a flow rate of 2 μL/min with a gradient of 10–45% of pump B in 90 min.

3.3 Identification of protein bearing bisected oligosaccharides

To identify proteins with altered glycans by the expression of GnT-III, we performed 2-DE followed by lectin blotting using PHA-E4 lectin, which recognizes bisecting GlcNAc in complex-type oligosaccharides. Although some bisected glycoproteins (70–120 kDa) could be visualized by 2-D lectin blotting, their expressions were too low to be detected on 2-DE gel. Lectin affinity chromatography, which is generally used for the concentration of glycoproteins, cannot be used for the insoluble fraction due to the presence of detergent in the solvent medium. Therefore, we first performed 1-D SDS-PAGE followed by lectin blotting, and then proteins in the range of 70–120 kDa were extracted from the gel (Fig. 4). 2-DE followed by lectin blotting was then performed, and interesting spots were successfully detected on 2-DE gel. Figure 5A and B shows the 2-DE gel images and the 2-D lectin blot of extracted proteins, respectively. The remarkable train spots (120 Da) of glycoprotein were picked up and in-gel digested with trypsin. The digest was subjected to LC/MS/MS, and the integrin α3 precursor was identified as the GnT-III target protein.

4 Discussion

The development of a simple and rapid method to explore glycan structural alteration in a complex mixture is required to elucidate the mechanisms of diseases involving glycan alteration. In this study, we demonstrated that GCC-LC/MS, which is used for glycosylation analysis in glycoproteins, is applicable for the exploration of changes in glycosylation between samples. Using GCC-LC/MS, high mannose, hybrid, and complex types as well as neutral and acidic oligosaccharides could be separated and characterized by a single analysis. GCC-LC/MS clearly shows differences in glycosylation between soluble and insoluble fractions. High mannose-type oligosaccharides were detected as major components in the soluble fraction. The soluble fraction contains endoplasmic reticulum and Golgi apparatus, where *N*-linked oligosaccharides are constructed. The predominance of high-mannose-type oligosaccharides in the soluble fraction may be the cause of immature oligosaccharides in the process of biosynthesis. In contrast, complex and hybrid types with or without sialic acids were detected in the insoluble fraction, suggesting that membrane proteins carry mature oligosaccharides.

In addition, GCC-LC/MS revealed differences in glycosylation between control cells and aberrant model cells. Biantennary forms bearing extra GlcNAc were obviously increased in cells transfected with the GnT-III gene, indicating that our methodology allows us to explore changes in the glycosyltransferase expression followed by glycan alteration. Although MS is frequently used for the analysis of glycosylation, identification of oligosaccharide isomers by MS alone

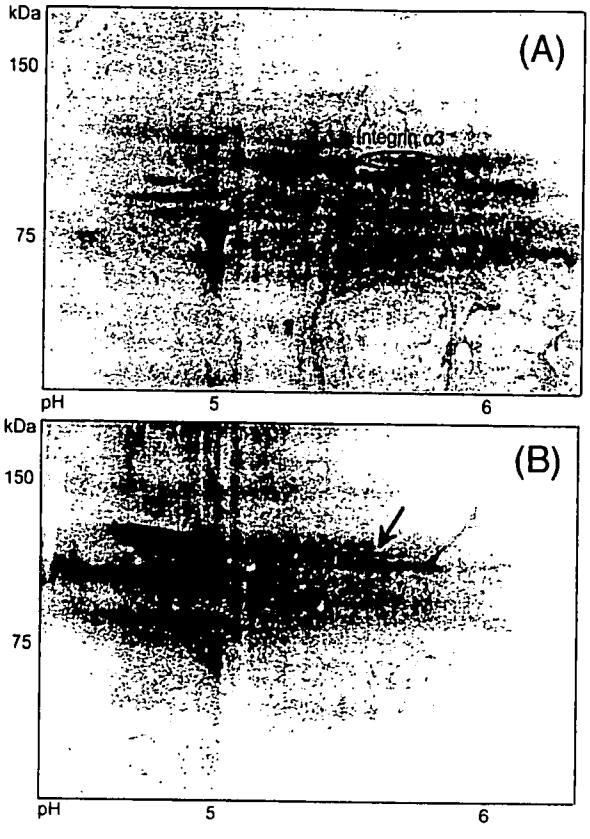

Figure 5. Enlarged partial (A) 2-DE and (B) lectin blot images from band A in Fig. 4.

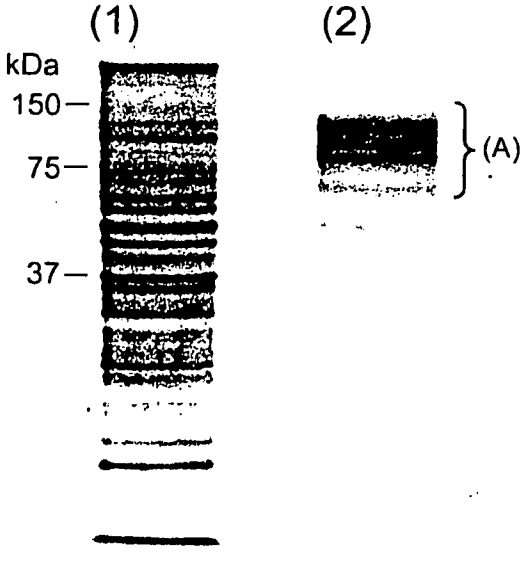

Figure 4. (1) 1-D SDS-PAGE and (2) lectin blot images of the CHO-III insoluble fraction. Proteins were separated on a 12.5% SDS-PAGE gel and stained with SYPRO Orange.

still remains challenges. Positional isomers could be differentiated by multiple-stage tandem mass spectrometry (MS^n); however, MS^n itself failed to identify oligosaccharides if the sample contained positional isomers. The use of GCC-LC/MS enables us to differentiate the structural isomers and perform differential analysis in glycosylation between normal and aberrant cells.

GnT-III is reported to involve the suppression of tumor cell metastasis and is assumed to be a marker of cancerous alteration in hepatic carcinoma [21, 22]. To identify the protein in which glycosylation was modified by GnT-III expression, we carried out 2-DE followed by lectin blotting, and Integrin α3 was identified as a target protein of GnT-III. Integrin α3, a type I membrane protein, is known to be a receptor of adhesion molecules, such as laminin 5 and 10/11 [23–25]. Our finding, in which integrin α3 is a target molecule of GnT-III, might be a clue to clarify the suppression mechanism of metastasis by GnT-III.

5 Concluding remarks

We propose a strategy for glycomic/glycoproteomic analysis using GCC-LC/MS in Fig. 6. First, GCC-LC/MS is used for oligosaccharide profiling to identify disease-related oligosaccharides. Based on the carbohydrate structure, appropriate lectins or antibodies could be selected for western blotting. Proteins carrying disease-related oligosaccharides could then be identified by 2-D lectin blotting followed by MS/MS analysis. Using several groups, 2-D lectin blotting has been proposed for the characterization of glycoproteins on gel [26, 27]. The use of mass spectrometric oligosaccharide profiling, which can directly characterize glycan structures, is worthwhile to obtain structural information about disease-related carbohydrate and is helpful in the subsequent choice of appropriate lectins and antibodies. Our method is expected to be a powerful tool for glycomic/glycoproteomic analysis.

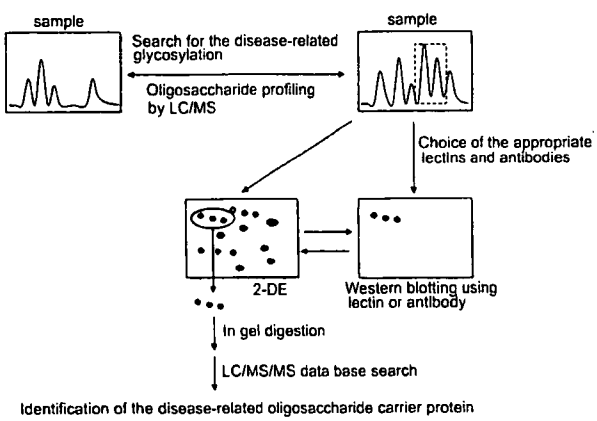

Figure 6. Strategy for glycomics/glycoproteomics using GCC-LC/MS, 2-DE and 2-D Western blotting using lectin or antibody.

6 References

[1] Varki, A., *Glycobiology* 1993, *3*, 97–130.

[2] Isaji, T., Gu, J., Nishiuchi, R., Zhao, Y. *et al.*, *J. Biol. Chem.* 2004, *279*, 19747–19754.

[3] Stanley, P., *Biochim. Biophys. Acta* 2002, *1573*, 363–368.

[4] Schachter, H., *Cell Mol. Life Sci.* 2001, *58*, 1085–1104.

[5] Dennis, J. W., Granovsky, M., Warren, C.E., *Biochim. Biophys. Acta* 1999, *1473*, 21–34.

[6] Delves, P. J., *Autoimmunity* 1998, *27*, 239–253.

[7] Gleeson, P. A., *Biochim. Biophys. Acta* 1994, *1197*, 237–255.

[8] Chui, D., Sellakumar, G., Green, R., Sutton-Smith, M. *et al.*, *Proc. Natl. Acad. Sci. USA* 2001, *98*, 1142–1147.

[9] Itoh, S., Kawasaki, N., Ohta, M., Hyuga, M. *et al.*, *J. Chromatogr. A* 2002, *968*, 89–100.

[10] Kawasaki, N., Haishima, Y., Ohta, M., Itoh, S. *et al.*, *Glycobiology* 2001, *11*, 1043–1049.

[11] Kawasaki, N., Ohta, M., Itoh, S., Hyuga, M. *et al.*, *Biologicals* 2002, *30*, 113–123.

[12] Davies, M., Smith, K. D., Harbin, A. M., Hounsell, E. F., *J. Chromatogr.* 1992, *609*, 125–131.

[13] Narasimhan, S., *J. Biol. Chem.* 1982, *257*, 10235–10242.

[14] Yoshimura, M., Ihara, Y., Matsuzawa, Y., Taniguchi, N., *J. Biol. Chem.* 1996, *271*, 13811–13815.

[15] Taniguchi, N., Miyoshi, E., Ko, J. H., Ikeda, Y., Ihara, Y., *Biochim. Biophys. Acta* 1999, *1455*, 287–300.

[16] Yoshimura, M., Nishikawa, A., Ihara, Y., Taniguchi, S., Taniguchi, N., *Proc. Natl. Acad. Sci. USA*.1995, *92*, 8754–8758.

[17] Bhaumik, M., Harris, T., Sundaram, S., Johnson, L. *et al.*, *Cancer Res.* 1998, *58*, 2881–2887.

[18] Laemmli, U. K., *Nature* 1970, *227*, 680–685.

[19] Stanley, S., Sundaram, S., Tang, J., Shi, S., *Glycobiology* 2005, *15*, 43–53.

[20] Lee, J., Sundaram, S., Shaper, N. L., Raju, S., Stanley, P., *J. Biol .Chem.* 2001, *276*, 13924–13934.

[21] Yamashita, K., Koide, N., Endo, T., Iwaki, Y., Kobata, A., *J. Biol. Chem.* 1989, *264*, 2415–2423.

[22] Yamashita, K., Hitoi, A., Taniguchi, N., Yokosawa, N. *et al.*, *Cancer Res.* 1983, *43*, 5059–5063.

[23] Carter, W. G., Ryan, M. C., Gahr, P. J., *Cell* 1991, *65*, 599–610.

[24] Kikkawa, Y., Umeda, M., Miyazaki, K., *J. Biochem (Tokyo)* 1994, *116*, 862–869.

[25] Kikkawa, Y., Sanzen, N., Sekiguchi, K., *J. Biol. Chem.* 1998, *273*, 15854–15859.

[26] Kim, Y. S., Hwang, S. Y., Oh, S., Shon, H. *et al.*, *Proteomics* 2004, *4*, 3353–3358.

[27] Rahman, M. A., Karsani, S. A., Othman, I., Rahman, P. S. A., Hashim, O. H., *Biochem. Biophys. Res. Commun.* 2002, *295*, 1007–1013.

Available online at www.sciencedirect.com
SCIENCE DIRECT
ELSEVIER
Journal of Chromatography A, 1094 (2005) 105–117
JOURNAL OF CHROMATOGRAPHY A
www.elsevier.com/locate/chroma

Characterization of a gel-separated unknown glycoprotein by liquid chromatography/multistage tandem mass spectrometry Analysis of rat brain Thy-1 separated by sodium dodecyl sulfate-polyacrylamide gel electrophoresis

Satsuki Itoh [a], Nana Kawasaki [a,b,*], Akira Harazono [a], Noritaka Hashii [a], Yukari Matsuishi [b], Toru Kawanishi [a], Takao Hayakawa [a]

[a] *Division of Biological Chemistry and Biologicals, National Institute of Health Science, 1-18-1, Kamiyoga, Setagaya-ku, Tokyo 158-8501, Japan*
[b] *CREST, Japan Science and Technology Agency (JST), Japan*

Received 17 May 2005; received in revised form 17 July 2005; accepted 25 July 2005
Available online 5 October 2005

Abstract

We developed an efficient and convenient strategy for protein identification and glycosylation analysis of a small amount of unknown glycoprotein in a biological sample. The procedure involves isolation of proteins by electrophoresis and mass spectrometric peptide/glycopeptide mapping by LC/ion trap mass spectrometer. For the complete glycosylation analysis, proteins were extracted in intact form from the gel, and proteinase-digested glycoproteins were then subjected to LC/multistage tandem MS (MS^n) incorporating a full mass scan, in-source collision-induced dissociation (CID), and data-dependent MS^n. The glycopeptides were localized in the peptide/glycopeptide map by using oxonium ions such as $HexNAc^+$ and $NeuAc^+$, generated by in-source CID, and neutral loss by CID-MS/MS. We conducted the search analysis for the glycopeptide identification using search parameters containing a possible glycosylation at the Asn residue with *N*-acetylglucosamine (203 Da). We were able to identify the glycopeptides resulting from predictable digestion with proteinase. The glycopeptides caused by irregular cleavages were not identified by the database search analysis, but their elution positions were localized using oxonium ions produced by in-source CID, and neutral loss by the data-dependent MS^n. Then, all glycopeptides could be identified based on the product ion spectra which were sorted from data-dependent CID-MS^n spectra acquired around localized positions. Using this strategy, we successfully elucidated site-specific glycosylation of Thy-1, glycosylphosphatidylinositol (GPI)-anchored proteins glycosylated at Asn23, 74, and 98, and at Cys111. High-mannose-type, complex-type, and hybrid-type oligosaccharides were all found to be attached to Asn23, 74 and 98, and four GPI structures could be characterized. Our method is simple, rapid and useful for the characterization of unknown glycoproteins in a complex mixture of proteins.

Keywords: Glycoprotein; LC/MS; Ion trap mass spectrometer; In-source CID; Thy-1

1. Introduction

Glycosylation is one of the most abundant post-translational modifications of proteins [1]. Most glycoproteins exist in heterogeneous forms due to their carbohydrate heterogeneity at multiple glycosylation sites. Because heterogeneity at each glycosylation site can be associated with many biological functions [2,3], it is necessary to analyze the oligosaccharide structures at each glycosylation site.

Mass spectrometric peptide/glycopeptide mapping by liquid chromatography coupled with electrospray ionaization tandem mass spectrometry (LC/ESI-MS/MS) is now used for characterization of glycoproteins [4,5]. Site-specific glycosylation of some gel-separated glycoproteins can be analyzed by in-gel proteinase digestion followed by MS; this method, however, gives unsatisfactory results due to a lower recovery of some glycopeptides from the gel [6–8]. For

* Corresponding author. Tel.: +81 3 3700 1141; fax: +81 3 3707 6950.
E-mail address: nana@nihs.go.jp (N. Kawasaki).

0021-9673/$ – see front matter © 2005 Elsevier B.V. All rights reserved.
doi:10.1016/j.chroma.2005.07.100

complete site-specific glycosylation analysis, all glycopeptide fragments should be recovered from the gel. Hence, the extraction of a whole glycoprotein from the gel before proteinase digestion would be more reasonable than in-gel digestion. Additionally, the poor ionization efficiency of glycopeptides makes it difficult to analyze the glycosylation of glycopeptides in a complex mixture of peptides [6,9]. The glycopeptide-specific method is required for mass spectrometric peptide/glycopeptide mapping.

A precursor ion scan using triple quadrupole-type mass spectrometer is favorably used for analysis of glycopeptides [10–13]. However, this method requires repetitive analysis for the protein identification and glycosylation analysis, as it monitors carbohydrate marker ions such as $HexNAc^+$ and $Hex\text{-}HexNAc^+$ fragmented from glycopeptides by collision-induced dissociation (CID)-MS/MS, and does not provide product ion spectra of non-glycosylated peptides. As such, additional analysis would not be possible for small quantities of proteins, including gel-separated glycoproteins. As an alternative method, we have previously demonstrated peptide/glycopeptide mapping using quadrupole time-of-flight mass spectrometer, by which product ions arise from both peptides and carbohydrates [14]. Using oxonium ions as marker ions, we can sort out product ion spectra of glycopeptides from a number of product ion spectra of peptides, and can determine the amino acid sequences of glycopeptides, glycosylation sites, and monosaccharide composition in a single analysis. Recently, ion trap mass spectrometry (ITMS), which is capable of data-dependent multistage tandem MS (MS^n), has been found to be preferable for use in glycosylation analysis of glycopeptides [15,16]. Glycopeptide-specific detection by precursor ion scan and data-dependent scan cannot be used for glycosylation analysis by ITMS due to the low mass cut-off system. Instead, oxonium ions fragmented by in-source CID are used for the localization of glycopeptides in the peptide/glycopeptide map [3,17]. It has recently been reported that peptide + GlcNAc ions originating from *N*-glycosylated peptides by MS^2 yield peptide b and y ions by further MS^n, and that the peptide sequence and *N*-glycosylation sites can be identified based on the peptide fragment ions [15,16,18]. In addition, another group has reported that glycopeptides can be identified in peptide/glycopeptide map by a search analysis using a database to which all possible cleavage products of the glycopeptides have been added in advance [19]. A combination of peptide/glycopeptide mapping with in-source CID, data-dependent CID-MS^n, and the database search analysis would enable protein identification, glycopeptide selection, and glycosylation analysis of a small amount of glycoprotein.

In the present study, we developed a strategy for the characterization of a small amount of unknown glycoprotein in a biological sample. An unknown glycoprotein was isolated by electrophoresis and extracted from the gel in an intact form. We used sodium dodecyl sulfate (SDS), which is effective for extracting proteins from the gel, and could be easily removed by adding cold acetone. The proteinase-digested glycoprotein was subjected to peptide/glycopeptide mapping, with the sequential scan consisting of a full mass scan, in-source CID, and data-dependent CID-MS^n. Using this method, we carried out site-specific glycosylation analysis of glycosylphosphatidylinositol (GPI)-anchored proteins in rat brain. A computer database search was used for the identification of a GPI-anchored protein and its *N*-glycosylation sites. In-source CID and data-dependent CID-MS/MS were also used for localization of peptides with *N*-glycan and GPI in the peptide/glycopeptide map. On the basis of their product ion spectra, we elucidated *N*-glycosylation at each glycosylation site and the structure of GPIs.

2. Experimental

2.1. Materials

Rat brains were purchased from Nippon SLC (Hamamatsu, Japan). Trypsin-Gold and endoproteinase Asp-N were purchased from Promega (Madison, WI, USA) and Wako Pure Chemical (Osaka, Japan), respectively. Phosphatidylinositol-specific phospholipase C (PIPLC) from *Bacillus cereus* were purchased from Molecular Probes (Eugene, OR, USA). All other chemicals used were of the highest purity available.

2.2. Sodium dodecyl sulfate-polyacrylamide gel electrophoresis (SDS-PAGE) of PIPLC-treated GPI-anchored proteins

PIPLC-treated GPI-anchored proteins were prepared from rat brain utilizing Triton X-114 phase partition and PIPLC digestion [20,21]. Two whole rat brains (2.8 g, Wistar, male, 3 weeks) were homogenized in cold acetone and centrifuged for 10 min at 4 °C. The precipitate was then homogenized in $CHCl_3$: methanol (2:1, v/v) and centrifuged for 10 min at 4 °C. After being washed with methanol, the pellet was homogenized in 50 mM Tris–HCl (pH 7.4) containing 150 mM NaCl, 1 mM ethylenediaminetetraacetic acid (EDTA), and 1 mM phenylmethylsulfonyl fluoride (PMSF), and centrifuged at 10,000 × *g* at 4 °C for 20 min. The pellet was resuspended in the same buffer with an additional 2% Triton X-114 (v/v), and stirred at 4 °C for 16 h. After centrifugation at 10,000 × *g* at 4 °C for 20 min, the supernatant was subjected to Triton X-114 phase-partitioning at 37 °C for 10 min. The detergent phase was resuspended with an equal volume of 50 mM Tris–HCl (pH 7.4) containing 150 mM NaCl. Solubilized membrane proteins in the detergent phase were precipitated with cold acetone and were resuspended in 400 μl of 50 mM Tris–HCl (pH 7.4). Following the addition of PIPLC (1 U), the suspension was incubated at 37 °C for 18 h. The suspension was resubjected to Triton X-114 phase-partitioning, and PIPLC-treated GPI-anchored proteins were precipitated with cold acetone from the aqueous phase. PIPLC-treated GPI-anchored proteins obtained from

50 mg of rat brain were separated by SDS-PAGE (12.5%) after carboxyamidomethylation [22].

2.3. Extraction and digestion of gel-separated proteins

The protein in gel band was extracted with 20 mM Tris–HCl containing 1% SDS by shaking vigorously overnight after breaking down the gel into small bits. The extract was filtered with Ultrafree-MC (0.22 μm, Millipore, Bedford, USA), and the protein was precipitated by adding cold acetone. The precipitate was digested with trypsin (1 μg) in 20 μl of 0.1 M Tris–HCl (pH8.0) at 37 °C for 16 h, or with Asp-N (0.4 μg) in 20 μl of 5 mM Tris–HCl (pH 7.5) at 37 °C overnight.

2.4. LC/MS^n

Proteolytic peptides were separated by a Magic C18 column (50 mm × 0.2 mm, 3 μm, Michrom BioResources, Auburn, CA, USA) with a Paradaim MS4 HPLC system (Michrom BioResources Inc., Auburn, CA, USA) consisting of pump A: 0.1% formic acid and 2% acetonitrile, and pump B: 0.1% formic acid and 90% acetonitrile. Separation was performed with a linear gradient of 5–65% of pump B in 40 min after 5% in 10 min of pump B at a flow rate 3 μl/min. Mass spectra were recorded by Finnigan LTQ (Thermo Electron, San Jose, CA, USA) with the sequential scan: a full mass scan (*m/z* 300–2000), a full mass scan with in-source CID (*m/z* 80–500, collision energy: 50 V), and data-dependent CID-MS^n for most intense ions at each scan with dynamic exclusion for 30 s. Scan time (*m/z* 300–2000) is approximately 0.1 s. The operating condition used for LC/ITMS was as follows: tube lens offset of 130 V, capillary voltage of 2.0 kV, capillary temperature of 200 °C.

2.5. Computer database search analysis

All product ions obtained by LC/ITMS were subjected to the computer database search analysis with the TurboSEQUEST search engine (Thermo Electron, San Jose, CA, USA). We used the NCBI database (rat, updated at February 2003) and following search parameters: a static modification of carboxyamidomethylation (57 Da) at Cys, a possible modification of GlcNAc (203 Da) at Asn, and trypsin used for digestion.

3. Results

3.1. Extraction of whole proteins from the gel

Rat brain PIPLC-treated GPI-anchored proteins were separated by SDS-PAGE (Fig. 1), and the most noticeable band at 20–25 kDa was cut off from the gel and crushed. The gel pieces were shaken vigorously in 1% SDS, and the extracted protein was precipitated with cold acetone to remove SDS.

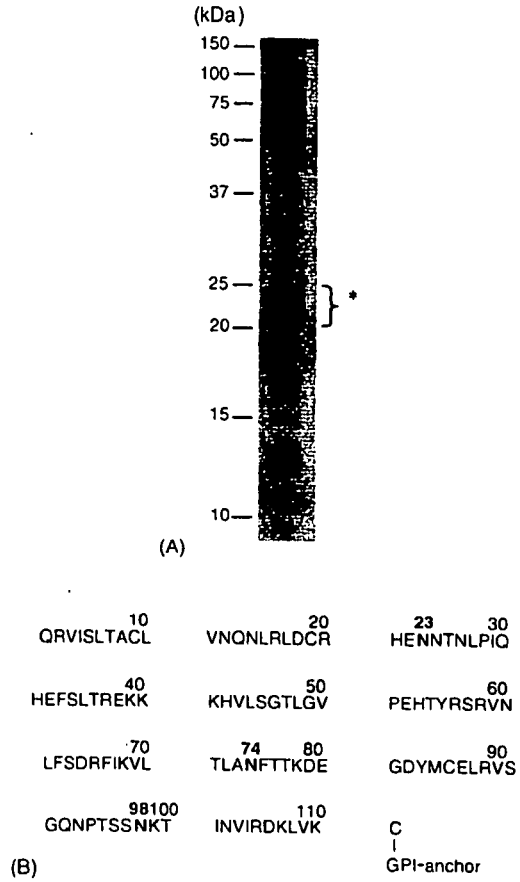

Fig. 1. (A) SDS-PAGE of PIPLC-treated GPI-anchored proteins from rat brain. (B) Amino acid sequence of rat Thy-1. *N*-Glycosylation sites are indicated by bold face. The protein at 20–25 kDa indicated by asterisk was subjected to the glycosylation analysis in this study.

We checked the recovery of the protein at 20–25 kDa by comparing the fluorescence intensity (Ex 633 nm/Em 670 nm) of the proteins at 20–25 kDa visualized by Coomassie staining before and after extraction. Approximately 55% of the protein at 20–25 kDa could be recovered from the gel (data not shown). The protein was digested with trypsin and subjected to the sequential scan consisting of full mass scans with and without in-source CID and data-dependent MS^n by LC/ITMS for protein identification and glycosylation analysis.

3.2. Database search analysis

Fig. 2(A) shows the peptide/glycopeptide map of the trypsin-digested protein at 20–25 kDa. First, all product ions generated by data-dependent MS^n were used for the database search analysis. Using search parameters described in Section 2.5, the protein was identified as Thy-1, a glycoprotein containing three *N*-glycosylation sites at Asn23, 74, and 98, and a GPI attachment site at Cys111. The search analysis also suggested the glycosylation at Asn74 and 98, with elution positions of 34 min (peak T6, Val69-Lys78) and 3.5 min (peak T1, Val89-Lys99), respectively (Fig. 2(A)). Although

Table 1
Glycosylation analysis of rat brain Thy-1

Glycosylation site	Carbohydrate composition[a]				Theoretical carbohydrate mass[b]	Trypsin					Asp-N				
	dHex	Hex	HexNAc	NeuAc		Observed *m/z*	Charge state	Peak number	Amino acid residue[c]	Theoretical *m/z*[b]	Observed *m/z*	Charge state	Peak number	Amino acid residue[c]	Theoretical *m/z*[b]
Asn23	0	5	2	0	1234.43	845.33	3	T3	H21-H31 (1315.63)	845.03	799.47	3	A3	E22-H31 (1178.57)	799.34
						937.27	3	T4	H21-F33 (1591.74)	937.06	1198.69	2	A3	E22-H31 (1178.57)	1198.50
						1405.81	2	T4	H21-F33 (1591.74)	1405.09	949.60	3	A3	N23-T36 (1626.80)	948.75
											1423.40	2	A3	N23-T36 (1626.80)	1422.62
	0	6	2	0	1396.49	899.49	3	T3	H21-H31 (1315.63)	899.04	853.54	3	A3	E22-H31 (1178.57)	853.36
						1348.35	2	T3	H21-H31 (1315.63)	1348.06	1279.66	2	A3	E22-H31 (1178.57)	1279.53
						942.16	3	T3	H21-E32 (1444.67)	942.06	1211.52	2	A5	E22-Q30 (1041.51)	1211.00
						991.37	3	T5	H21-F33 (1591.74)	991.08					
						1486.40	2	T5	H21-F33 (1591.74)	1486.12					
	0	3	5	0	1519.57						1044.43	3	A3	N23-T36 (1626.80)	1043.79
	0	7	2	0	1558.54	996.41	3	T3	H21-E32 (1444.67)	996.07	907.59	3	A3	E22-H31 (1626.80)	907.37
											1361.03	2	A3	E22-H31 (1178.57)	1360.56
	1	3	5	0	1665.62						1093.32	3	A3	N23-T36 (1626.80)	1092.48
	1	5	4	0	1786.65						1133.80	3	A3	N23-T36 (1626.80)	1132.82
	0	6	3	1	1890.66						1168.51	3	A4	N23-T36 (1626.80)	1167.49
	1	6	4	0	1948.70						1187.21	3	A3	N23-T36 (1626.80)	1186.84
Asn74	1	2	3	0	1405.52	1026.26	3	T6	V59-F75 (1996.12)	1026.18					
	0	5	2	0	1234.43	949.52	2	T2	A73-K78 (680.35)	949.39	995.71	3	A7	D64-K78 (1766.01)	995.15
						1162.72	2	T6	V69-K78 (1106.62)	1162.53					
	1	4	3	0	1421.52	1043.45	2	T2	A73-K78 (680.35)	1042.94					
	1	3	4	0	1462.54	1063.68	2	T2	A73-K78 (680.35)	1063.45					
						1276.61	2	T6	V69-K78 (1106.62)	1276.58					
	1	5	3	0	1583.57	1124.18	2	T2	A73-K78 (680.35)	1123.96					
						1337.64	2	T6	V69-K78 (1106.62)	1337.10					
	1	3	5	0	1665.62	1165.13	2	T2	A73-K78 (680.35)	1164.99	1272.15	2	A4	T71-K78 (894.48)	1272.05
						919.71	3	T6	V69-K78 (1106.62)	919.09	1139.79	3	A7	D64-K78 (1766.01)	1138.88
						1378.19	2	T6	V69-K78 (1106.62)	1378.12					
	2	5	3	0	1729.63	1197.53	2	T2	A73-K78 (680.35)	1196.99					
	2	4	4	0	1770.66	1217.67	2	T2	A73-K78 (680.35)	1217.51					
						1430.71	2	T6	V69-K78 (1106.62)	1430.64					
	1	5	4	0	1786.65	1226.38	2	T2	A73-K78 (680.35)	1225.50					
						960.01	3	T6	V69-K78 (1106.62)	959.43					
						1439.05	2	T6	V69-K78 (1106.62)	1438.64					
	1	4	5	0	1827.68	973.79	3	T6	V69-K78 (1106.62)	973.10					
	2	5	4	0	1932.71	1298.75	2	T2	A73-K78 (680.35)	1298.53	1228.18	3	A7	D64-K78 (1766.01)	1227.91
						1008.71	3	T6	V69-K78 (1106.62)	1008.11					
						1512.21	2	T6	V69-K78 (1106.62)	1511.67					
	1	6	4	0	1948.70	1306.81	2	T2	A73-K78 (680.35)	1306.53					
						1013.98	3	T6	V69-K78 (1106.62)	1013.45					
	0	4	5	1	1972.71						1241.91	3	A7	D64-K78 (1766.01)	1241.25
	2	4	5	0	1973.73	880.04	3	T2	A73-K78 (680.35)	879.70	1241.84	3	A7	D64-K78 (1766.01)	1241.59
						1319.24	2	T2	A73-K78 (680.35)	1319.04					
						1022.43	3	T6	V69-K78 (1106.62)	1021.79					
						1532.49	2	T6	V69-K78 (1106.62)	1532.49					

	1	6	3	1	2036.72	1043.24	3	T7	V69-K78 (1106.62)	1042.78					
	1	5	4	1	2077.75	1057.08	3	T7	V69-K78 (1106.62)	1056.46					
	2	6	4	0	2094.76	1062.65	3	T6	V69-K78 (1106.62)	1062.13	1282.43	3	A7	D64-K78 (1766.01)	1281.93
	1	4	5	1	2118.77	1070.38	3	T7	V69-K78 (1106.62)	1070.14					
	2	5	5	0	2135.79	1076.32	3	T6	V69-K78 (1106.62)	1075.81					
	1	6	4	1	2239.80	1110.97	3	T7	V69-K78 (1106.62)	1110.48					
	3	5	5	0	2281.85	1124.78	3	T6	V69-K78 (1106.62)	1124.49					
	1	7	5	0	2313.84	851.76	4	T6	V69-K78 (1106.62)	851.62					
	1	4	6	1	2321.85	1138.16	3	T7	V69-K78 (1106.62)	1137.83					
	2	5	6	1	2629.96	1241.13	3	T7	V69-K78 (1106.62)	1240.53					
Asn98	0	5	2	0	1234.43	1168.34	2	T1	V89-K99 (1117.54)	1167.99	912.24	3	A2	E86-K99 (1515.76)	911.74
											1367.31	2	A2	E86-K99 (1515.76)	1367.10
											930.26	3	A3	Q92-R105 (1570.84)	930.10
											1021.28	3	A3	E86-N102 (1843.94)	1021.13
											1011.53	3	A4	T95-K110 (1815.06)	1010.81
											1516.43	2	A4	T95-K110 (1815.06)	1516.75
											1144.21	3	A5	E86-R105 (2212.18)	1143.88
	0	3	4	0	1316.49	1209.79	2	T1	V89-K99 (1117.54)	1209.02					
	0	3	5	0	1519.57	1310.68	2	T1	V89-K99 (1117.54)	1310.56	1007.10	3	A2	E86-K99 (1515.76)	1006.78
											1106.39	3	A4	T95-K110 (1815.06)	1106.55
											1239.21	3	A5	E86-R105 (2212.18)	1238.92
	2	3	4	0	1608.60						951.28	3	A4	G91-N102 (1259.61)	951.08
											1426.22	2	A4	G91-N102 (1259.61)	1426.11
	1	4	4	0	1624.60	951.37	3	T3	S96-D106 (1245.67)	951.76					
	0	5	4	0	1640.59	1371.84	2	T1	V89-K99 (1117.54)	1371.07	960.04	4	A5	E86-R105 (2212.18)	959.70
											1279.69	3	A5	E86-R105 (2212.18)	1279.26
	0	5	3	1	1728.61						1176.27	3	A4	T95-K110 (1815.06)	1176.23
	0	5	4	0	1640.59						1146.70	3	A4	T95-K110 (1815.06)	1146.89
	1	6	3	0	1745.62						1082.52	3	A2	E86-K99 (1515.76)	1082.13
											1181.80	3	A4	T95-K110 (1815.06)	1181.90
											986.38	4	A5	E86-R105 (2212.18)	985.96
											1314.72	3	A5	E86-R105 (2212.18)	1314.27
	1	5	4	0	1786.65						1195.47	3	A4	T95-K110 (1815.06)	1195.57
											996.54	4	A5	E86-R105 (2212.18)	996.21
											1328.49	3	A5	E86-R105 (2212.18)	1327.95
	1	5	3	1	1874.67						1018.89	4	A6	E86-R105 (2212.18)	1018.22
	0	6	3	1	1890.66	1496.18	2	T1	V89-K99 (1117.54)	1496.10	1230.24	3	A4	T95-K110 (1815.06)	1230.24
											1022.70	4	A6	E86-R105 (2212.18)	1022.22
	2	5	4	0	1932.71	1517.35	2	T1	V89-K99 (1117.54)	1517.13					
	1	6	4	0	1948.70	1525.78	2	T1	V89-K99 (1117.54)	1525.12	1150.13	3	A2	E86-K99 (1515.76)	1149.83
											1249.75	3	A4	T95-K110 (1815.06)	1249.59
											1259.45	3	A3	E86-N102 (1843.94)	1259.22
											1037.27	4	A5	E86-R105 (2212.18)	1036.73
											1382.34	3	A5	E86-R105 (2212.18)	1381.97
	1	6	3	1	2036.72						1059.07	4	A6	E86-R105 (2212.18)	1058.73
	0	6	4	1	2093.74						1298.06	3	A4	T95-K110 (1815.06)	1297.94
											1073.37	4	A6	E86-R105 (2212.18)	1072.99

[a] dHex, deoxyhexose; Hex, hexose; HexNAc, *N*-acetylhexosamine; NeuAc, *N*-acetylneuramic acid.

[b] Monoisotopic value.

[c] Theoretical peptide mass is indicated in parenthesis.

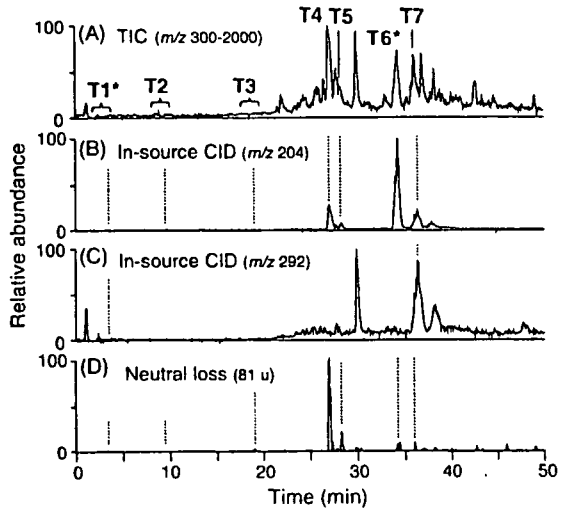

Fig. 2. Total ion chromatogram (TIC) of trypsin-digested protein at 20–25 kDa (*m/z* 300–2000) (A), mass chromatograms from TIC with ion-source CID of *m/z* 204 (B) and 292 (C), and neutral loss chromatogram of 81 u by data-dependent CID-MS/MS (D). Asterisks mean the peak of glycopeptides identified by the database search analysis.

the glycopeptide Val89-Lys99 contains two Asn residues, Asn93 and 98, only Asn98 was identified as a glycosylation site because of detection of b and y ions modified with GlcNAc at Asm98.

Next, to study the site-specific glycosylation at Asn74 and 98, product ion spectra of glycopeptides were sorted from the numbers of product ion spectra acquired around peak T6 and T1. We sorted out product ion spectra of glycopeptides using B series ions, such as $Hex_1HexNAc_1^+$ and $Hex_2HexNAc_1^+$ (*m/z* 366 and 528) originated from glycopeptides by CID-MS/MS, as marker ions [23]. We could sort out 14 product ion spectra originated from glycopeptide Val69-Lys78 around peak T6. The monosaccharide compositions of *N*-glycans at Val69-Lys78 were calculated as $dHex_{0-3}Hex_{2-7}HexNAc_{2-5}$ on the basis of the *m/z* values of their molecular ions and the theoretical mass of the peptide. Likewise, seven product ion spectra originated from glycopeptide Val89-Lys99 were sorted from those around peak T1, and their monosaccharide compositions were estimated as $dHex_{0-2}Hex_{3,5,6}HexNAc_{2-5}NeuAc_{0,1}$ (Table 1). Glycosylation at Asn74 and 98 were elucidated by a detailed examination of these product ion spectra as follows.

3.2.1. Analysis of the glycosylation at Asn74 of peptide Val69-Lys78

Fig. 3(A) shows a product ion spectrum of the glycopeptide Val69-Lys78 at 34.52 min. Its precursor ion is the doubly charged ion at *m/z* 1512.2. Many product ions generated by cleavages of glycosidic linkages can be observed in this product ion spectrum. The most intense ion at *m/z* 1311 is assigned to a peptide bearing the reducing end of GlcNAc, which was caused by glycosidic linkage cleavage of *N*-linked oligosaccharide. Fig. 3(B) is the product ion spectrum of the peptide + GlcNAc ion at *m/z* 1311. The b and y ions generated by cleavages of the peptide backbone prove that this glycopeptide is the peptide Val69-Lys78 glycosylated at Asn74.

The molecular weight of the carbohydrate moiety can be calculated as 1933.8 Da by subtracting the theoretical mass of the peptide (1106.6 Da) from the calculated glycopeptide mass (3022.4 Da). Consequently, the monosaccharide composition can be estimated as $dHex_2Hex_5HexNAc_4$. In the product ion spectrum (Fig. 3(A)), B ions corresponding to $dHex_1Hex_1HexNAc_1$ ($B_{2\alpha}$) and $dHex_1Hex_2HexNAc_1$ ($B_{3\alpha}$) were detected at *m/z* 512 and 674, respectively. These results indicate that one of two dHex, which are likely to be Fuc, attaches to Gal-GlcNAc at the non-reducing end in a similar manner as the Lewis a/x antigen (Gal-(Fuc-)GlcNAc-), or the blood group H-determinant (Fuc-Gal-GlcNAc-). The product ion at *m/z* 350 produced from the triply charged precursor ion at *m/z* 1008.7 corresponded to $dHex_1HexNAc_1$ (data not shown), suggesting that Fuc attaches to GlcNAc like the Lewis a/x antigen (Gal-(Fuc-)GlcNAc-). The attachment site of the other Fuc can be deduced at inner trimannosyl core GlcNAc from the observation of Y ions at *m/z* 1457, 1660, and 1822, which correspond to Val69-Lys78 plus $dHex_1HexNAc_1$ ($Y_{1\alpha}$), $dHex_1HexNAc_2$ ($Y_{2\alpha}$), and $dHex_1Hex_1HexNAc_2$ ($Y_{3\alpha/3\beta/3\gamma}$), respectively. In addition, the product ion at *m/z* 1411 resulting from the precursor ion at *m/z* 1512.2 by loss of 101.6 u (HexNAc), suggests a linkage of non-substituted HexNAc at the non-reducing terminal end. Together with detection of the product ion at *m/z* 940 ($Y_{3\alpha/1\beta/3\beta}^+$, [GlcNAc-Man-GlcNAc-GlcNAc-peptide+H]$^{2+}$), it can be deduced that this HexNAc is a bisecting GlcNAc attached to the core mannose residue via a β1–4 linkage. From these product ions, we could deduce two oligosaccharide structures. One is the structure indicated in Fig. 3(A), inset, and the other is one containing a Gal-Gal-(Fuc-)GlcNAc-Man-branch instead of a Gal-(Fuc-)GlcNAc-Man-branch. Detection of Gal-(Fuc-)GlcNAc-Man$^+$ at *m/z* 674 but not Gal-Gal-(Fuc-)GlcNAc-Man$^+$ at *m/z* 836 suggests that this oligosaccharide structure can be assigned to the structure indicated in Fig. 3(A), inset.

The carbohydrate structures of the other glycopeptide Val69-Lys78 detected around peak T6 can be characterized as the high-mannose-type oligosaccharide (M5), complex-type oligosaccharides containing some partial structures such as inner core Fuc, bisecting GlcNAc, the Lewis a/x antigen, and blood group H-determinant, and hybrid-type oligosaccharides (Table 1).

3.2.2. Analysis of the glycosylation at Asn98 of peptide Val89-Lys99

Fig. 4 shows one of the product ion spectra of the glycopeptide Val89-Lys99 at 3.47 min. Its precursor ion is the doubly charged ion at *m/z* 1525.8. The monosaccharide composition, $dHex_1Hex_6HexNAc_4$, can be estimated based on the calculated mass of the carbohydrate moiety (1950.0 Da) obtained by subtracting the mass of the theo-

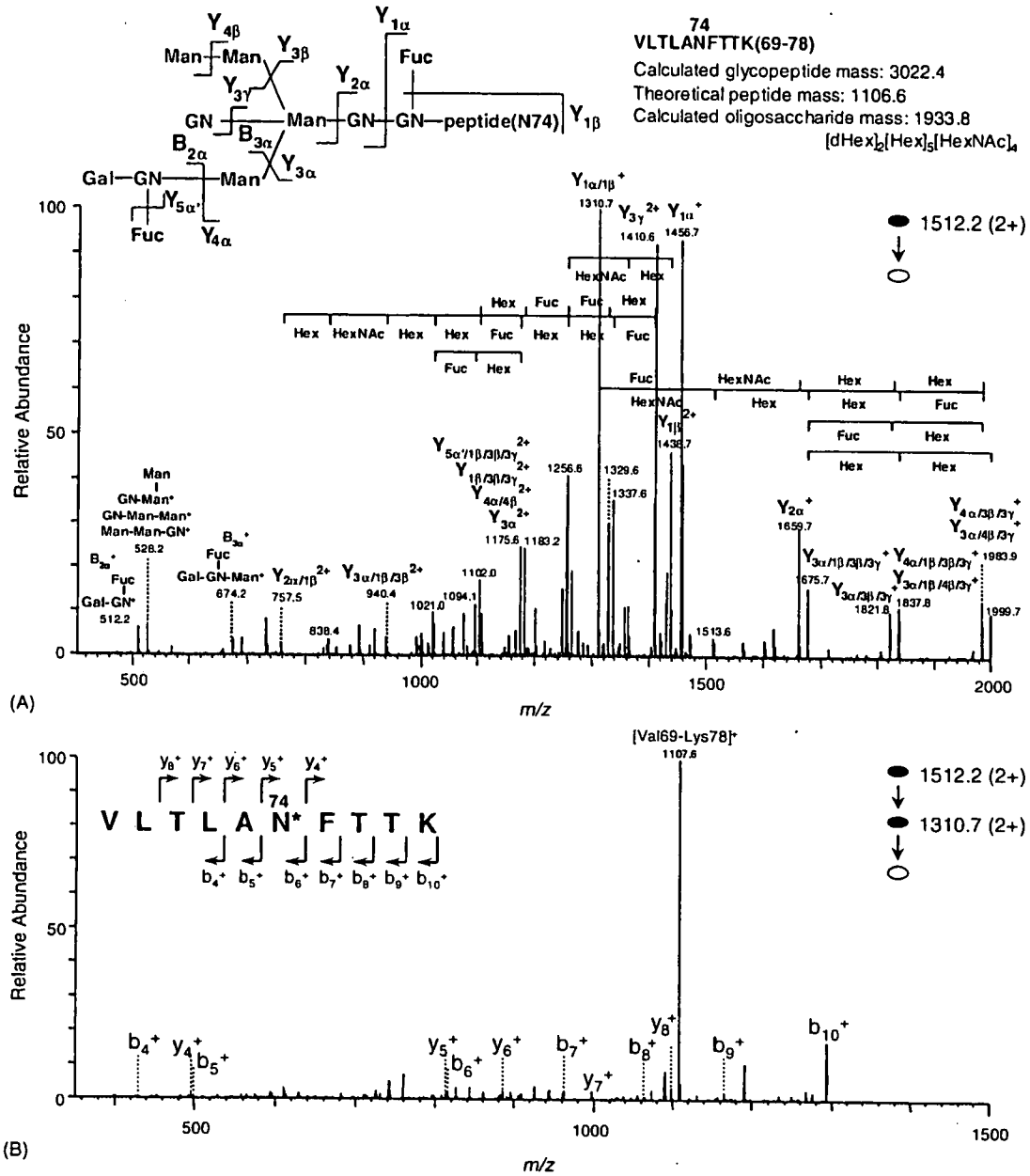

Fig. 3. (A) Product ion spectrum (MS^2) of the doubly charged glycopeptide precursor ion at *m/z* 1512.2 in peak T6. The glycopeptide Val69-Lys78 is glycosylated with oligosaccharide, $dHex_2Hex_5HexNAc_4$ at Asn74, and the inset is the deduced oligosaccharide structure. (B) MS^3 product ion spectrum derived from the doubly charged glycopeptide precursor ion at *m/z* 1512.2, followed by further fragmentation of the product ion at *m/z* 1310.7.

retical typtic peptide mass (1117.5 Da) from the calculated glycopeptide mass (3049.5 Da). Y ions corresponding to Val89-Lys99 plus $dHex_1HexNAc_1$ ($Y_{1\alpha}$), $dHex_1HexNAc_2$ ($Y_{2\alpha}$), and $dHex_1Hex_1HexNAc_2$ ($Y_{3\alpha/3\beta/3\gamma}$) detected at *m/z* 1468, 1671, and 1833, respectively, reveals that one Fuc residue is linked to the inner trimannosyl core GlcNAc. Additionally, the product ion at *m/z* 1424 suggests a linkage of non-substituted HexNAc at the non-reducing terminal end. Together with the product ions at *m/z* 945 and 1890, it can be deduced that this HexNAc is a bisecting GlcNAc that attaches to a core mannose residue via a β1–4 linkage. On the basis of the product ions at *m/z* 487, 528 and 1380, corresponding to Hex_3 ($B_{2\beta}$), $Hex_2HexNAc_1$ ($B_{3\alpha}$), and $Hex_6HexNAc_2$ ($B_{4\alpha}$), the oligosaccharide structure was characterized as a hybrid-type oligosaccharide (Fig. 4, inset).

The carbohydrate structures of the other glycopeptide Val89-Lys98 detected around peak T1 are characterized as high-mannose-type oligosaccharide (M5), complex-type, and hybrid-type oligosaccharides, which include bisecting GlcNAc and Lewis a/x structures (Table 1).

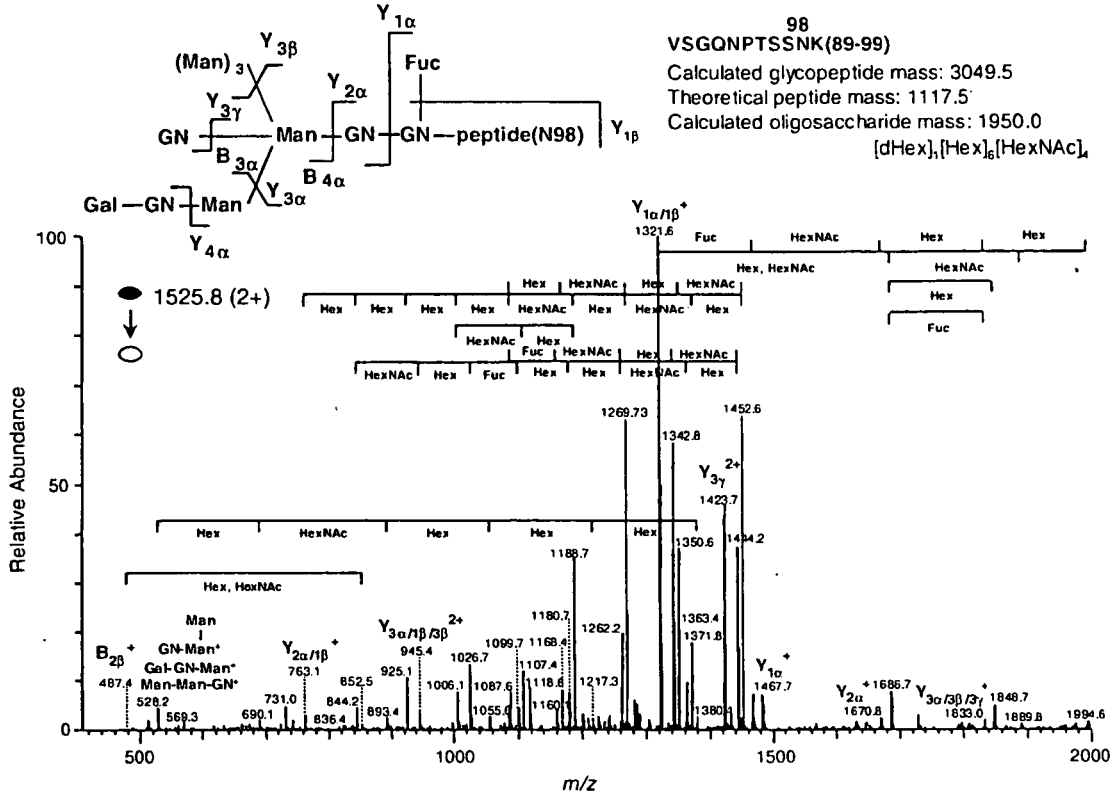

Fig. 4. Product ion spectrum of the doubly charged glycopeptide precursor ion at *m/z* 1525.8 in peak T1. The glycopeptide Val89-Lys99 is glycosylated with the oligosaccharide, $dHex_1Hex_6HexNAc_4$ at Asn98, and the inset is the deduced oligosaccharide structure.

3.3. Detection of glycopeptides by in-source CID and CID-MS/MS

Glycopeptides containing Asn23 could not be identified by the database search analysis. Therefore, we first localized all glycopeptides in the peptide/glycopeptide map using oxonium marker ions generated by in-source CID. Fig. 2(B and C) shows mass chromatograms of oxonium marker ions, $HexNAc^+$ (*m/z* 204) and $NeuAc^+$ (*m/z* 292), respectively. The mass chromatogram of *m/z* 204 indicates that the glycopeptides were localized around 3.7, 9.7, 19.1, 27.2, 28.4 34.3, 36.3, and 37.8 min. The mass chromatogram of *m/z* 292 suggests that the glycopeptides bearing NeuAc were localized around 3.7, 30.0, 36.4, and 38.2 min. In addition to the localization of glycopeptides by in-source CID, we monitored neutral loss caused by data-dependent CID-MS/MS. The neutral loss chromatogram of 81 u indicates the localization of doubly charged glycopeptides ions with Hex at the non-reducing ends. The elution positions of the localized glycopeptides by neutral loss are almost identical to those by in-source CID. Second, for confirmation of the elution position of glycopeptides and characterization of the carbohydrate moiety, we sorted the product ion spectra of glycopeptides from enormous numbers of data-dependently acquired product ion spectra around localized glycopeptides by using oligosaccharide oxonium ions as marker ions. Consequently, the locations of glycopeptides were confirmed in peak T1-6 (Fig. 2(A)). The peaks T1 and 6 correspond to the location of glycopeptides identified by the database search as Val89-Lys99 and Val69-Lys78, respectively. Four glycopeptide peaks were newly sorted by in-source CID and data-dependent CID-MS/MS. Structural assignment of the glycopeptides in these peaks was carried out using their MS^n spectra as follows.

3.3.1. Analysis of the glycosylation at Asn23 of peptide His21-Phe33

Fig. 5(A) shows one of the product ion spectra of the glycopeptide His21-Phe33 in peak T4. Its precursor ion is the triply charged ion at *m/z* 937.3. The intense product ion at *m/z* 899 is assigned to a doubly charged ion of peptide plus GlcNAc on the basis of Y series ions. The region of His21-Phe33 containing Asn23 in Thy-1 was suggested as the peptide moiety of this glycopeptide, 1593.3 Da, by the FindPept tool available on the internet (ExPASY Proteomics tools, Swiss Institute of Bioinformatics, http://us.expasy.org/tools/findpept.html). We examined the data-dependently acquired product ion spectrum of the precursor ion at *m/z* 899 and found that the *m/z* values of b and y ions in the product ion spectrum were identical to those of predictable product ions originating from the peptide His21-Phe33 modified with HexNAc at Asn23 (Fig. 5(B)). From the calculated oligosaccharide mass (1235.1 Da) obtained by subtracting the theoretical typtic

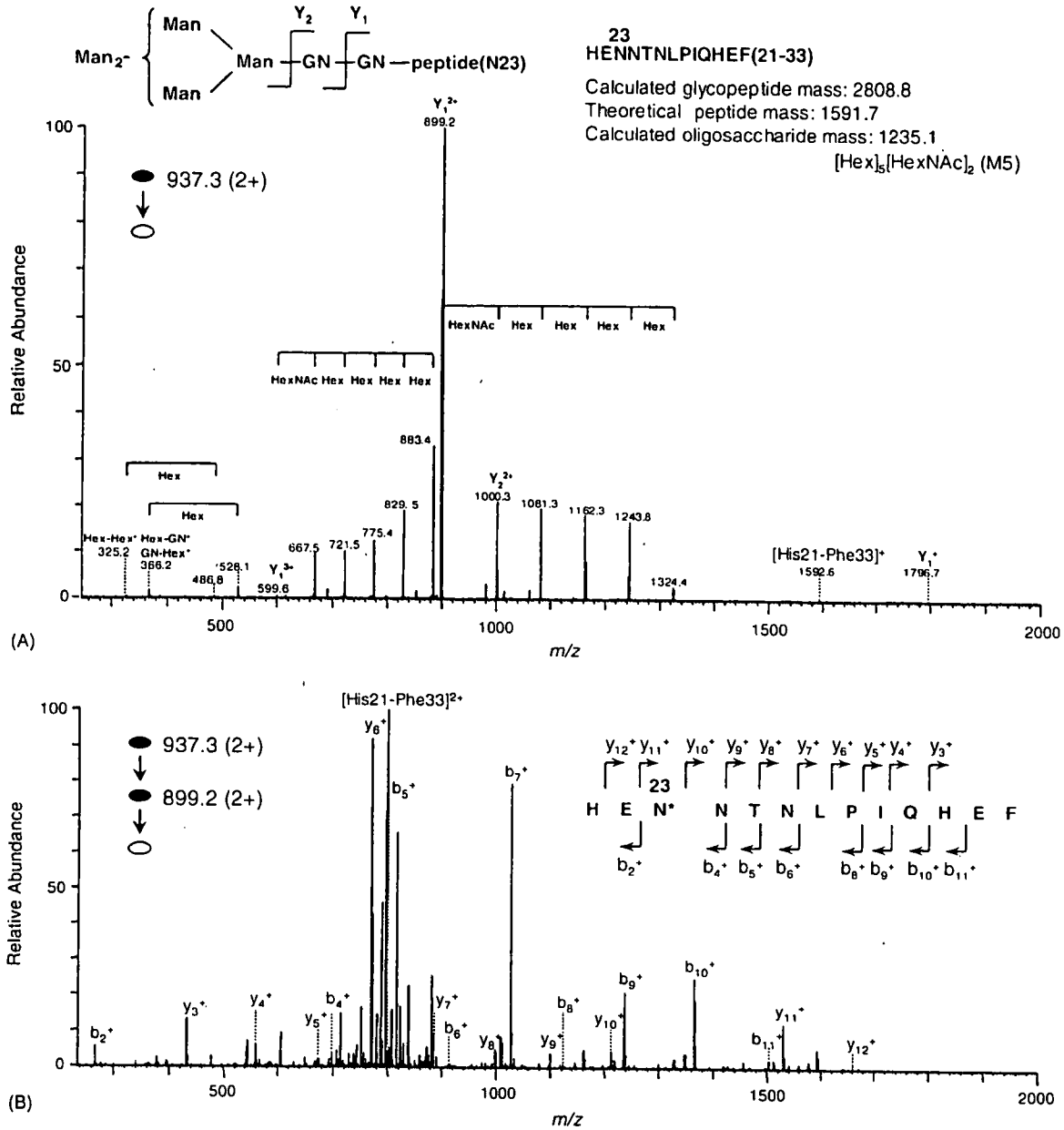

Fig. 5. (A) Product ion spectrum (MS^2) of the doubly charged glycopeptide precursor ion at *m/z* 937.3 in peak T4. The glycopeptide His21-Phe33 is glycosylated with oligosaccharide, $Hex_5HexNAc_2$ at Asn23, and the inset is the deduced oligosaccharide structure. (B) MS^3 product ion spectrum derived from a doubly charged glycopeptide precursor ion at *m/z* 937.3, followed by further fragmentation of the product ion at *m/z* 899.2.

peptide mass (1591.7 Da) from the calculated glycopeptide mass (2808.8 Da) together with product ions at *m/z* 366 and 528, it is indicated that this peptide carries $Hex_5HexNAc_2$, i.e. high-mannose-type oligosaccharide, M5. All product ion spectra in peak T4 revealed that peptides His21-Phe33 contain only high-mannose-type oligosaccharide (M5).

3.3.2. *Analysis of glycopeptides in peaks T2, 3, 5, and 7*

Similarly, product ion spectra of glycopeptides around peaks T2, 3, 5, and 7 were sorted by using oligosaccharide oxonium marker ions generated by MS/MS. In product ion spectra sorted out from around peak T2, the intense ion at *m/z* 884 was detected and assigned to a singly charged ion of a peptide plus GlcNAc. The peptide was suggested to be Ala73-Lys78 containing Asn74 by the FindPept tool. The monosaccharide composition can be estimated from the calculated mass of oligosaccharide moiety obtained by subtracting the theoretical mass of Ala73-Lys78 (680.35 Da) from calculated glycopeptide mass. Oligosaccharide structure of the glycopeptides is characterized based on their product

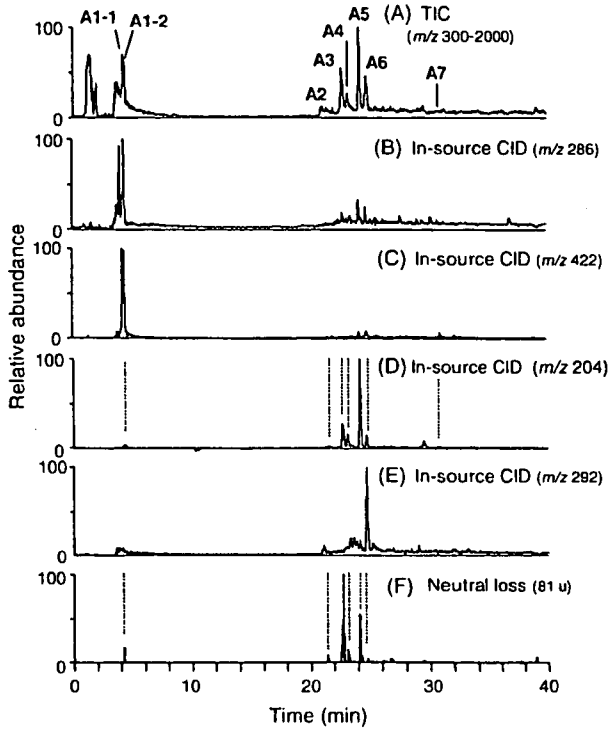

Fig. 6. Total ion chromatogram (TIC) of Asp-N digested protein at 20–25 kDa (*m/z* 300–2000) (A), mass chromatograms from TIC with in-source CID of *m/z* 286 (B), 422 (C), 204 (D), and 292 (E), and neutral loss chromatogram of 81 u by data-dependent CID-MS/MS (F).

ion spectra. Glycopeptides in peak T2 were characterized as Ala73-Lys78 glycosylated at Asn74 with *N*-glycans consisting of $dHex_{0-2}Hex_{3-6}HexNAc_{2-5}$. These *N*-glycans can be identified as high-mannose-type oligosaccharide (M5), and complex-type and hybrid-type oligosaccharides containing Fuc attached to inner trimannosyl core GlcNAc. Their structural assignments are summarized in Table 1. Glycopeptides in peak T3 can be identified as a mixture of peptide His21-His31 and His21-Glu32 glycosylated at Asn23, and Ser96-Asp106 glycosylated at Asn98. Asn23 was attached by high-mannose-type oligosaccharides, M5, 6, and 7, and Asn98 was occupied by *N*-glycan consisting of $dHex_1Hex_4HexNAc_4$ with a Lewis a/x structure as a partial structure. Glycopeptides in peak T5 were characterized as peptide His21-Phe33 glycosylated at Asn23 with high-mannose-type oligosaccharide, M6. Glycopeptides in peak T7 were assigned to be Val69-Lys78 glycosylated at Asn74 with *N*-glycans composed of $dHex_{1-2}Hex_{4-6}HexNAc_{3-6}NeuAc$.

3.4. Analysis of the GPI moiety of rat Thy-1

Since trypsin digestion provided Cys-GPI, which could not be retained on the C_{18} column, Asp-N digestion was also performed to obtain more hydrophobic peptides attached by GPI (GPI-peptides). Fig. 6(A) shows the peptide/glycopeptide map obtained by LC/ITMS of Asp-N digested Thy-1. We localize the GPI-peptides using marker ions, EtN-PO_4-Man$^+$ at *m/z* 286 and GlcN-inositol-PO_4^+ at *m/z* 422, originating from the core structure of the GPI moiety by in-source CID (EtN, ethanolamine; GlcN, glucosamine). Mass chromatograms of *m/z* 286 and 422 suggest the locations of the GPI-peptides to be around 4.2 (peak A1-1) and 4.4 min (peak A1-2) (Fig. 6(B and C)). Using product ions originated from GPI moiety, such as GlcN-inositol-PO_4^+ and PO_4-Man-GlcN$^+$ (*m/z* 422 and 404), as marker ions, four product ion spectra of GPI-peptides were sorted out from all product ion spectra around peaks A1-1 and 1-2. Their precursor ions were doubly charged ions at *m/z* 1132 and 1213 (peak A1-1), 1051 and 1151 (peak A1-2). Based on these product ion spectra, we characterized GPI-peptides as the peptide Asp106-Cys111 with a GPI core structure plus Hex_{0-2}, $HexNAc_{1-2}$ and PO_4-EtN.

Fig. 7(A) shows the product ion spectrum of the doubly charged GPI-peptide ion at *m/z* 1051 in peak A1-2. In addition to product ions at *m/z* 422, those originating from the GPI moiety were detected at *m/z* 404 (PO_4-Man-GlcN$^+$), 447 (EtN-PO_4-Man-GlcN$^+$), 650 (EtN-PO_4-(HexNAc-)Man-GlcN$^+$), 787 (peptide-EtN$^+$), 868 (peptide-EtN-PO_4^+), 1191 (peptide-EtN-PO_4-Man-Man$^+$), 1477 (peptide-EtN-PO_4-Man-Man-(EtN-PO_4-)Man$^+$), 1638 (peptide-EtN-PO_4-Man-Man-(EtN-PO_4-)Man-GlcN$^+$), and 1898 (peptide-EtN-PO_4-Man-Man-(EtN-PO_4-)Man-GlcN-inositol-PO_4^+). From these fragments, it can be deduced that this peptide is Asp106-Cys111 carrying the GPI, as indicated in the inset in Fig. 7(A).

The other GPI-peptide in peak A1-1 was characterized as having side chains; -Hex attached to M1, -PO_4-EtN and -HexNAc attached to M3, based on the product ion spectrum of the doubly charged precursor ion at *m/z* 1132 (data not shown). These two GPI structures are identical to those that have been previously reported [24].

Product ion spectra of doubly charged ion at *m/z* 1151 and 1213 suggested that they contained GPI which bear one HexNAc or two Hex in addition to GPI in Fig. 7(A) respectively. Fig. 7(B) shows the product ion spectra of the doubly charged precursor ions at *m/z* 1151 in peak A1-2. In addition to *m/z* 422, we detected product ions at *m/z* 366 (HexNAc-Man$^+$), 447 (EtN-PO_4-Man-GlcN$^+$), 650 (EtN-PO_4-(HexNAc-)Man-GlcN$^+$), 1229 (peptide-EtN-PO_4-(HexNAc-)Man$^+$), 1391 (peptide-EtN-PO_4-(HexNAc-)Man-Man$^+$), 1676 (peptide-EtN-PO_4-(HexNAc-)Man-Man-(EtN-PO_4-)Man$^+$), 1838 (peptide-EtN-PO_4-(HexNAc-)Man-Man-(EtN-PO_4-)Man-GlcN$^+$), and 1880 (peptide-EtN-PO_4-(HexNAc-)Man-Man-(EtN-PO_4-)(HexNAc-)Man$^+$). These fragment ions suggest the attachment of -HexNAc to Man1, and -PO_4-EtN and -HexNAc to Man3 as indicated in the inset of Fig. 7(B). Similarly, product ion spectra of the doubly charged precursor ion at *m/z* 1213 indicate the attachment of 2Hex and HexNAc to Man1 and Man3-PO_4-EtN (data not shown). To our knowledge, this is the first report of these two GPI structures in Thy-1.